Since January 2020 Elsevier has created a COVID-19 resource centre with free information in English and Mandarin on the novel coronavirus COVID-19. The COVID-19 resource centre is hosted on Elsevier Connect, the company's public news and information website.

Ecological Informatics 69 (2022) 101675

Contents lists available at ScienceDirect

Ecological Informatics

journal homepage: www.elsevier.com/locate/ecolinf

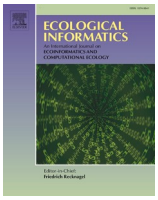

Habitat distribution change of commercial species in the Adriatic Sea during the COVID-19 pandemic

Gianpaolo Coro [a,*], Pasquale Bove [a], Anton Ellenbroek [b]

[a] Istituto di Scienza e Tecnologie dell'Informazione "Alessandro Faedo" – CNR, Pisa, Italy
[b] Food and Agriculture Organization of the United Nations, Viale delle Terme di Caracalla, 00153 Rome, Italy

ARTICLE INFO

Keywords:
Ecological niche modelling
Marine science
COVID-19
Conservation biology

ABSTRACT

The COVID-19 pandemic has led to reduced anthropogenic pressure on ecosystems in several world areas, but resulting ecosystem responses in these areas have not been investigated. This paper presents an approach to make quick assessments of potential habitat changes in 2020 of eight marine species of commercial importance in the Adriatic Sea. Measurements from floating probes are interpolated through an advection-equation based model. The resulting distributions are then combined with species observations through an ecological niche model to estimate habitat distributions in the past years (2015–2018) at 0.1° spatial resolution. Habitat patterns over 2019 and 2020 are then extracted and explained in terms of specific environmental parameter changes. These changes are finally assessed for their potential dependency on climate change patterns and anthropogenic pressure change due to the pandemic. Our results demonstrate that the combined effect of climate change and the pandemic could have heterogeneous effects on habitat distributions: three species (*Squilla mantis*, *Engraulis encrasicolus*, and *Solea solea*) did not show significant niche distribution change; habitat suitability positively changed for *Sepia officinalis*, but negatively for *Parapenaeus longirostris*, due to increased temperature and decreasing dissolved oxygen (in the Adriatic) generally correlated with climate change; the combination of these trends with an average decrease in chlorophyll, probably due to the pandemic, extended the habitat distributions of *Merluccius merluccius* and *Mullus barbatus* but reduced *Sardina pilchardus* distribution. Although our results are based on approximated data and reliable at a macroscopic level, we present a very early insight of modifications that will possibly be observed years after the end of the pandemic when complete data will be available. Our approach is entirely based on Findable, Accessible, Interoperable, and Reusable (FAIR) data and is general enough to be used for other species and areas.

1. Introduction

The COVID-19 pandemic has directly affected human activities in many world areas (Coro and Bove, 2022), but its direct and indirect effects on the ecosystems of these areas are still under study. The reduced anthropogenic pressure on these ecosystems may have been beneficial for species habitats. However, the combined effects of the pandemic and climate change may have triggered complex reactions. Analysing natural pattern changes can reveal how ecosystems have responded to general climatic trends and inter-annual climatic variations within the context of human pressure reduction in 2020. In particular, marine ecosystems, especially in the Adriatic Sea, have benefited from the reduction of stress factors such as (i) fishing and vessel traffic (Depellegrin et al., 2020), (ii) disturbance of species life (Kemp et al., 2020), (iii) nutrient load in coastal areas (Adwibowo, 2020; Mishra et al., 2020; Shehhi and Samad, 2021), and (iv) water pollution (Yunus et al., 2020). Understanding these benefits is interesting to quantitatively assess the peculiar marine ecosystem dynamics modifications that occurred at various levels (e.g., pollution, biodiversity, and ecosystems) and how these influenced human activities (e.g., fisheries, ecosystem services, social interaction and mobility, and illegal activities) (Snapshot-CNR, 2020). Understanding these dynamics allows identifying correlations that would have been hidden without the lockdowns and help designing novel strategies for marine resource sustainability. For example, the lockdowns have allowed scientists to better model the resilience of Adriatic fishing fleets to activity closure, i.e., the time to return to regime fishing activity and market saturation (Coro et al., 2022). Moreover, the 2020 lockdown restrictions to fishing

* Corresponding author.
E-mail addresses: coro@isti.cnr.it (G. Coro), pasquale.bove@isti.cnr.it (P. Bove), anton.ellenbroek@fao.org (A. Ellenbroek).

https://doi.org/10.1016/j.ecoinf.2022.101675
Received 11 January 2022; Received in revised form 10 May 2022; Accepted 11 May 2022
Available online 21 May 2022

activities in many areas (including the Adriatic) have limited scientific survey ranges and resulted in missing survey hauls with consequent information loss on stock biomass in 2020. This scenario calls for solutions to estimate biomass variation in 2020 despite the data gaps, which in turn requires information about habitat modification as support to expert observations, biomass estimates, and fishing catch change understanding (Brown et al., 2010; Coro et al., 2020, 2021; Trifonova et al., 2017; Weatherdon et al., 2016).

This paper analyses the potential habitat change, in 2020, of eight marine species of commercial importance in the Adriatic Sea: European hake (*Merluccius merluccius*), common sole (*Solea solea*), mantis shrimp (*Squilla mantis*), red mullet (*Mullus barbatus*), common cuttlefish (*Sepia officinalis*), European anchovy (*Engraulis encrasicolus*), European pilchard (*Sardina pilchardus*), and deep-water rose shrimp (*Parapenaeus longirostris*). These species are target of beam (common sole, mantis shrimp, common cuttlefish), bottom (red mullet, deep-water rose shrimp, European hake), and mid-water (European anchovy and pilchard) trawlers and purse seine vessels (European anchovy and pilchard). They currently account for about 70% of the total catch in the basin (FAO, 2020). The related fishing grounds range from coastal and offshore waters to deeper waters (e.g., the Pomo Pit) (Russo et al., 2020). The high fishing stress on these species and most Adriatic stocks (Froese et al., 2018) makes them relevant to understand how the combination of reduced anthropogenic stress during the COVID-19 pandemic and climatic changes influenced their distribution in the Adriatic. The study presented in this paper sheds light on the magnitude of change in one year of reduced anthropogenic pressure. Additionally, it indicates the sensitivity of the species' habitats to environmental change and can be used to predict the economic and ecological impact of a return to the pre-pandemic human activity level.

Habitat assessment often estimates the *ecological niche* of a species (Coro et al., 2016a; Deneu et al., 2021; Jones et al., 2012; Weber et al., 2017), i.e., the set of resources and environmental conditions that foster its persistence and proliferation in an area. It indicates such conditions either in the species' native habitat (native niche) or in other geographical areas (potential niche). Mathematically, a species' ecological niche is the space within a hyper-volume, in a vector space made up of environmental parameters, associated to the species' proliferation. Ecological niche models (ENMs) both estimate the parameters to use in the vector space and identify the hyper-volume boundaries. As a first step, an ENM uses statistical analysis or machine learning to estimate a predictive function between species observation records and specific environmental parameters. As a second step (projection phase), it applies the predictive function to other environmental parameter values that refer to a new area or other environmental scenarios (Peterson et al., 2007). For example, a model trained on the environmental parameters of an area in 2015 can be projected onto the parameter values in 2020 (Coro, 2020; Coro et al., 2018c). In the experiment presented in this paper, individual ENMs for the eight selected species were estimated for average environmental parameter values of the 2015–2018 years. Then they were projected onto the environmental parameters of 2020 to see if the COVID-19 related changes influenced habitat distribution change. Furthermore, the major parameters driving change were checked against other studies to assess if the observed variations potentially depended on climate change (rather than inter-annual climatic variations) or the pandemic. Our experiment was conducted in a context of minimal environmental and species-occurrence data available for the pandemic period. Information extraction techniques were therefore used to estimate enough information to feed the ENMs. Pattern recognition was finally used to infer habitat change information over the years.

ENMs have been used to identify suitable areas for species (Menchetti et al., 2019; Peterson, 2003). The generality of the approach made them adopted in early predictions of the potential spread of COVID-19 due to environmental and meteorological conditions, e.g., they foresaw the lower summer outbreak rate of 2020 (Araujo and Naimi, 2020; Coro, 2020). These models have demonstrated a sufficient prediction effectiveness when working with few data, for example to predict rare species distributions (Chunco et al., 2013; Coro et al., 2013a, 2015b; de Siqueira et al., 2009). The possibility to process environmental parameters over time also makes them effective to monitor long-term habitat change (Ashraf et al., 2017; Ben Rais Lasram et al., 2010; Chala et al., 2019; Coro et al., 2016a, 2018c; Friedlaender et al., 2011). ENMs commonly require uniformly distributed environmental parameters estimated from real observations over the study area. These distributions can result from hydrodynamic models based on point observations coming from satellite (Alvera-Azcárate et al., 2005; Durand et al., 2010; Werdell and Bailey, 2005) or in situ probes (Huang et al., 2008; Peterson, 2001; Ravdas et al., 2018; Scarponi et al., 2018). Effective distributions are also obtainable through lower-complexity models, based on the advection equation that simulates the dispersion of a quantity by currents (Djakovac et al., 2015; Lipizer et al., 2014; Troupin et al., 2012). Parameters estimated from these models commonly find applications in ecological models (Blackford, 2002; Garcia et al., 2019; Toonen and Bush, 2020) and ecological niche models (Azzolin et al., 2020; Coll et al., 2007). Accurate parameter selection is also integral to ENMs, because these models are sensitive to mutually-dependent variables and achieve higher performance when using independent variables (Pearson, 2007). A correct variable selection is typically achieved through statistical analysis (Guo and Liu, 2010; Magliozzi et al., 2019; Muscarella et al., 2014; Sánchez-Tapia et al., 2017; Schnase et al., 2021) or other ENMs (Warren and Seifert, 2011; Coro et al., 2013a, 2015b,a; Zeng et al., 2016; Bargain et al., 2017).

This paper proposes a workflow based on the application of ENMs to in situ environmental parameter observations and expert-verified species observations to discover habitat change across 2015–2018, 2019, and 2020. The 2015–2018 period was used as an aggregated and meaningful reference for average environmental conditions and species presence in the near past, and 2019 data were used to assess if the variations observed in 2020 were due to the pandemic or climate change. First, punctual environmental observations were transformed into uniform parameter distributions through an advection equation-based model. Second, parameter selection per species was conducted to feed ENMs with the parameters mostly associable with the species habitat (e.g., its preferred depth range and environmental conditions). Third, the consistency of our ENMs was verified against other ENMs calculated independently. Fourth, habitat variation over the years, per species, was studied to identify habitat change trends. Finally, these trends were explained in terms of environmental parameter change potentially correlated with climate change and the pandemic. Our study used only a few, but reliable, environmental and species data. This choice was made to investigate the viability of open data and thus to only use actual observations whose modulations contained information on the reduced anthropogenic pressure in 2020 due to the pandemic.

Our analysis identified robust patterns at the Adriatic scale but cannot be considered punctually reliable because it is based on few data (i.e., it is a data-poor approach). Nevertheless, it offers an unprecedented possibility to shed light on the modifications that the combined action of the COVID-19 pandemic and climate change brought to species' distribution in the Adriatic Sea, way ahead of the time when data will be collected, collated, and analysed after the end of the pandemic. The open data approach was possible thanks to the recent investments by international communities on Findable, Accessible, Interoperable, and Reusable (FAIR) data, Open Science, and data collection networks addressing the realisation of digital twins of marine systems (EU Commission, 2020b).

2. Methods

2.1. Data

Our experiment used the data of the international Argo float network

(Argo, 2000). This network includes robotic probes that drift with ocean currents while moving and measuring biogeochemical parameters along the water column. These probes collect environmental information with sampling frequencies ranging from 2 s to several minutes, reaching down to 2000 m in 10-day data collection cycles. Data streams are transmitted via satellite to distributed information centres (Global Data Assembly Centers, GDACs). GDACs make the data freely available for download (Argo, 2000). Argo currently exposes over 20-years of data and manages ~4000 operational floats. Floats are located worldwide except for ice zones, with a higher density in the equatorial belt. The collected environmental parameters include depth, pressure, dissolved oxygen, ocean-current speed components, practical salinity, temperature, wind-stress components, electrical conductivity, chlorophyll-a, and fluorescence. Argo data can be included in the class of FAIR data as being free, timely, and unrestricted-access data (Tanhua et al., 2019). Data access has the only policy to acknowledge the Argo network in scientific publications. Ethical oversight is left to the individual scientists or organizations using the data.

To use Argo data in our niche models, they were aggregated and processed to reduce noise and computational complexity. Three groups of data were selected and downloaded from the GDACs - in CSV format - for the Adriatic Sea (using a bounding box extension of [+8;+20] longitude and [+38;+46] latitude). The first dataset contained observations from 2015 to 2018; the second included observations collected in 2019; the third contained observations collected in 2020. The 2015–2018 range represents an aggregated reference of environmental conditions in the near past. This aggregation was necessary to provide reference statistical averages for the environmental parameters and allowed collecting a meaningful set of species observations for training ENMs. The 2019 data were used as a reference to assess if the variations observed in 2020 were either due to the pandemic or continuing trends from the previous years (possibly related to climate change). The 2020 data were assumed to contain observations with signals of the COVID-19 pandemic and climate change.

Argo data were averaged at a 0.1° resolution to increase statistical viability (Coro et al., 2018b). The following parameters were extracted from the CSV data: temperature (°C), salinity (PSU), chlorophyll-a (mg/m^3), dissolved oxygen (DOX) ($\mu mol/kg$). These are indeed the most abundant and reliable data downloadable from Argo. For each parameter, average values were calculated for surface range, seafloor (bottom), and the entire water column. Surface and bottom ranges were identified as the first and last ranges of a logarithmic division, into five parts, of the maximum depth of each 0.1° cell in the Adriatic (Coro et al., 2018b; Reyes, 2015). Instead of using static ranges, this approach adapted the definition of surface and bottom ranges to the specific cell depth. It normally results in better niche modelling, especially for benthic and demersal species (Ready et al., 2010; Reyes, 2015). For each parameter, surface, bottom, and average (in the water column) values were estimates at 0.1° resolution. Furthermore, locations outside of the Adriatic Sea were excluded by only using those within the geographical subareas 17 and 18 of the General Fisheries Commission for the Mediterranean (GFCM, 2020). This process generated 36 datasets overall, as the results of three aggregation types (surface, bottom, average), for each aggregation time (2015–2018, 2019, 2020), repeated for four parameters.

As a final step, consistency between the observations from the different datasets was enhanced by constraining all datasets to cover the same areas. Different spatial coverage over the years can indeed be a source of bias. For example, if observations covered north Adriatic more extensively than south Adriatic in a particular year, sampling would be northward skewed with consequent over-representation of northern environmental values. If this is not the case for the other years, inconsistency between parameter sampling and representation will occur. To avoid this issue, only probes locations that were present in all reference years were retained. A 0.5° spatial tolerance was used in the selection of these locations.

The ENM used in the present experiment required environmental data uniformly distributed over the Adriatic Sea. Consequently, all 0.1° cells required an environmental value assigned, either averaged from the Argo observations or estimated through a model. Given the low density and quantity of the available environmental observations (Section 3) and the importance of currents in the biogeochemical components' drift and spread in the Adriatic, parameter values were interpolated through a model based on the advection equation and depth information. In particular, the Data-Interpolating Variational Analysis (DIVA) was used (Barth et al., 2010). DIVA is commonly used to produce uniform distributions of environmental parameters (Coro et al., 2018a; Coro and Trumpy, 2020; Schaap and Lowry, 2010) and solves the advection equation to simulate the transport of a substance or quantity by currents. DIVA also estimates the mutual spatial correlation between observations and requires minimal parametrisation to produce high-quality interpolation at a user-defined resolution (Coro et al., 2016c; Troupin et al., 2010, 2012). Internally, DIVA reconstructs a continuous field from discrete measurements through a numerical implementation of the Variational Inverse Model (Bennett, 1992). This algorithm fits a continuous field to the data through a minimization cost function (Watelet et al., 2016), using a finite-element statistical method that embeds topographic and dynamic constraints (based on bathymetry and oceanic-currents data). It can process irregularly-spaced observations to produce estimates on a regular grid. Based on this fit, DIVA estimates a triangular-element mesh over the interpolation area, where the characteristic length of each element is directly linked to the mutual spatial correlation between observations.

For our experiment, DIVA was applied to all Argo-aggregated data described in Section 2.1. Data of ocean current components were taken as NetCDF files from the Global Ocean Physic Analysis dataset hosted by the Copernicus Marine Service (Von Schuckmann et al., 2018). In addition, depth information was taken from the GEBCO-2020 bathymetry dataset, a global terrain model for ocean and land with 0.0042° uniform spatial resolution (GEBCO, 2020). To execute DIVA, the D4Science e-Infrastructure computational platform was used (Assante et al., 2019; Candela et al., 2016; Coro et al., 2015a, 2017). As a result, 36 uniform parameter distributions at 0.1° resolution for our environmental parameter aggregations were produced and represented with the ESRI-grid format (ASC).

2.2. Species observations

In order to extract species observation data, we consulted the Ocean Biogeographic Information System (OBIS) (Grassle, 2000). OBIS contains taxonomic and occurrence information for ~155,000 marine species and provides access to more than 163 million observation records, integrated from more than 4000 sources. Its contributors include international research projects, national monitoring programs, museums, and individuals. OBIS is suitable for data mining and pattern recognition experiments, especially in data-poor scenarios where the quality of the data is fundamental to produce reliable analyses (Coro et al., 2013b, 2015c, 2016b, 2018c). The OBIS data quality checking is integral to ecological niche models that are particularly sensitive to data bias (Coro et al., 2015b). Furthermore, for each occurrence record, OBIS indicates if it underwent expert verification. This feature makes OBIS more suited for ecological niche modelling in data-poor scenarios than other data collections (Coro et al., 2015b, 2015c). In our experiment, the OBIS observation records in the Adriatic Sea, between 2015 and 2018, that underwent expert verification were retrieved for the eight species under study. Their coordinates were stored as CSV files to feed ENMs later.

2.3. Ecological niche modelling

Maximum Entropy (MaxEnt) is a widely used ENM for marine species (Angeletti et al., 2020; Capezzuto et al., 2018; Raybaud et al., 2015).

MaxEnt is a shallow machine learning model that estimates a function $\pi(\overline{x})$ defined over real-valued vectors $\overline{x}$ of environmental parameters. This function is forced to reach maxima on the parameters associated with a species' presence and minima on absence-related parameters. Following a common abuse of notation, $\pi(\overline{x})$ can be considered a proxy of a probability density of a species' presence given the $\overline{x}$ environmental parameters (Elith et al., 2011; Merow et al., 2013; Phillips and Dudík, 2008). MaxEnt learns the relation between environmental values in the species-observation locations and the general species' presence (Coro et al., 2018c; Pearson, 2007). One advantage of this model is that it can work with species-presence information only, but it is over-sensitive to biased data (Coro et al., 2015b; Elith and Graham, 2009). A MaxEnt model trained with parameters and species observations at 0.1° resolution will produce a probability distribution of species presence over the 0.1° cell subdivision of a study area. The $\pi(\overline{x})$ function is thus the probability that a 0.1° cell is suitable species habitat. MaxEnt estimates $\pi(\overline{x})$ after maximising the entropy function $H = -\sum \pi(\overline{x})\ ln(\pi(\overline{x}))$ on the training locations with respect to randomly-selected environmental parameter vectors in the study area (*background points*). In the present experiment, $\overline{x}$ was made up of 13 parameters associated with the 2015–2018 year range: temperature, salinity, chlorophyll-a, DOX (with related surface, bottom, water-column aggregations), and depth (from the GEBCO-2020 bathymetry data set). Although depth was constant through the years, it was included in our models because it is a fundamental parameter to estimate the niches of the studied species correctly. Depth was used as a proxy to model species preference to different seabeds and water column heights. Thus, it enhanced prediction reliability by adding complementary and valuable information about the species habitat. On the other hand, it was not functional to the subsequent pattern analysis. Training locations were those associated with the OBIS observations between 2015 and 2018. The used MaxEnt implementation (Phillips et al., 2021) accepted environmental parameters in ASC-raster format and species observation data in CSV format.

The training algorithm estimates the coefficients of a linear combination of the environmental parameters. These coefficients represent the weight of each environmental parameter in the species' environmental preferences (*percent contribution*). MaxEnt also estimates the *permutation importance* of each parameter in the $\overline{x}$ vector. The training process is based on the following function definitions: $f(\overline{x})$, the probability density over the background parameters; $f_1(\overline{x})$, the density on the training set; and *pr*, the prior distribution (*prevalence*) of the species (equal to 0.5 when no prior assumption is available, as in our case). Based on these functions, $\pi(\overline{x})$ is defined as

$$\pi(\overline{x}) = \frac{f_1(\overline{x}) \cdot pr}{f(\overline{x})}$$

In a maximum entropy condition, the optimal $f_1(\overline{x})$ is the closest function to $f(\overline{x})$, because there would be no difference without species observations. Additionally, $f_1(\overline{x})$ should have maxima on the parameter means in the training set locations. With these constraints, the model minimises the Kullback-Leibler distance between $f_1(\overline{x})$ and $f(\overline{x})$

$$d(f_1(\overline{x}), f(\overline{x})) = \sum_{\overline{x}} f_1(\overline{x}) \cdot log_2\left(\frac{f_1(\overline{x})}{f(\overline{x})}\right)$$

This minimisation is solved by Gibbs distribution functions in the form $f_1(\overline{x}) = f(\overline{x}) e^{\eta(\overline{x})}$ (Phillips et al., 2006a), with $\eta(\overline{x}) = \alpha + \beta\ h(\overline{x})$; α being a normalization constant that makes $f_1(\overline{x})$ sum to 1; h being an optional transformation of $\overline{x}$ that simulates a complex relation between the environmental parameters; and β being the *percent contribution* coefficients. The minimisation of $\eta(\overline{x})$ - which requires solving a log-linear equation - consequently minimises $d(f_1(\overline{x}), f(\overline{x}))$. The used MaxEnt software automatically solves this minimisation problem. It also estimates percent parameter contribution through an iterative process that calculates and accumulates the percent performance gain provided by each parameter (Phillips et al., 2017).

MaxEnt is generally preferred over linear and logistic regression for species habitat distribution modelling. It is equivalent to a Poisson regression (a generalized linear model) that is naturally suited for modelling the probability of a number of events in a fixed space (such as species occurrences) (Renner and Warton, 2013). Once the model parameters have been estimated, the $\pi(\overline{x})$ function can be used to estimate probability distributions over new parameter values than those of the training set, e.g. the parameters of locations outside of the study area (to discover the potential species niche) or new environmental scenarios (to study niche change over time) (Elith and Graham, 2009; Phillips et al., 2017).

MaxEnt is sensitive to sampling bias associated with species-observation locations and can over-fit small datasets (Merow et al., 2013; Wang et al., 2018). Our selected occurrence datasets were indeed small, as only expert-verified records were selected. They also had potentially biased distributions, as they belonged to OBIS-included surveys with frequent and fixed paths (Coro et al., 2015c). One way to manage this issue is to select background points far away from the presence locations (Hengl et al., 2009). However, our analysed species are common and widely distributed in the Adriatic, with absence locations potentially dense in the presence areas. Therefore, it was not possible to focus background point sampling on specific areas. Providing the model with precise absence and background locations would also have required more presence data and precise environmental parameter distributions. However, specific studies on MaxEnt parametrisation (Dudík et al., 2005; Phillips et al., 2017; Phillips and Dudík, 2008; Zaniewski et al., 2002) have indicated general strategies to reduce presence location sampling and over-fitting biases, which include (i) selecting background points to reflect the same sampling bias as the presence locations, (ii) including presence points among background points, (iii) using *hinge* features to model complex species response to the environmental parameters and make model fitting more flexible. The MaxEnt software used for this experiment offers options to use *hinge* features and include presence locations among background points if these are associated with unique combinations of environmental parameters (Phillips et al., 2021). These options were used to attenuate over-fitting and sampling bias issues as far as possible.

In the present experiment, MaxEnt was trained with 2015–2018 Adriatic environmental data and species occurrence records to produce an ecological niche reference for the near past. Then it was projected onto the 2019 and 2020 environmental data to analyse probability distribution change due to the different environmental parameters of these years. Since the β vector indicates the parameters that carry the highest quantity of information to understand species habitat preferences (Coro, 2020; Coro et al., 2018c), it can be used to remove poorly niche-correlated parameters from the $\overline{x}$ vector. This operation optimally selects the variables associated with the species habitat (Section 3.1). For example, deep-water and benthic species will likely be modelled with bottom-averaged parameters, whereas pelagic species habitat will likely be modelled with water-column or surface related parameters. Furthermore, reducing the number of input environmental parameters decreases the inter-dependence between the variables and improves the model accuracy (Coro et al., 2015b). In the present experiment, the MaxEnt models of the studied species were first trained with all parameters and then re-trained using only those parameters having a *percent contribution* within 95% from the maximum contribution.

In summary, MaxEnt ENMs were produced for the 8 Adriatic species through the following steps: (i) MaxEnt models were trained with 2015–2018 OBIS observations and interpolated environmental data; (ii) after a first training phase, the parameters with the 95% highest *percent contributions* were retained (thus, different parameter sets were associated to the different species); (iii) the models were re-trained only with the retained parameters; (iv) the models were projected onto the 2019 and 2020 environmental parameters. The produced models will be referred to as *floating sensor* (FS) based models - i.e., FS 2015–2018, FS 2019, and FS 2020 - to distinguish them from the baseline models used

for evaluation. A total of 24 models was thus produced, i.e., three models for each analysed species.

2.4. Evaluation and pattern recognition

The ENM distributions were used to discover driving factors of species habitat change over the years. The first goal of our quality evaluation was to assess the consistency of the produced maps. As our second goal, the principal environmental drivers of habitat suitability change were checked against evidence from general climate change and COVID-19 pandemic related trends. The entire evaluation process was managed through four *evaluation questions*:

2.4.1. Question 1: Are the produced distributions consistent?

This question was answered by verifying the similarity between our models and other ENMs. This operation confirmed that our models consistently captured the species' environmental preferences, although they were trained on scarce and scattered data and tested on the same training set (Section 3.1). Indeed, the partial reliability of our MaxEnt model was assessed using the training data, but this was insufficient to state they were consistent, due to the few data at hand. Thus, we set two consistency boundaries for our model: one similarity and one dissimilarity reference. We used the similarity reference to confirm that the produced distributions agreed with an independent habitat distribution. Instead, we used the dissimilarity reference to check for significant difference with respect to a known improbable scenario based on unlikely environmental parameter distributions.

The AquaMaps distributions were used for these tasks (Kaschner et al., 2006). They were downloaded (not re-calculated) from the AquaMaps website (AquaMaps, 2020). AquaMaps is a presence-only ENM that incorporates scientific expert knowledge into species habitat modelling to account for known limitations of species occurrence records (Corsi et al., 2000; Ready et al., 2010). We used AquaMaps as a mechanistic model to estimate species distributions independently of the data available in our experiment. Moreover, AquaMaps uses a complementary approach with respect to machine-learning-based approaches because it explicitly models the causality between species presence and environmental parameters (Baker et al., 2018; Pearson, 2007). AquaMaps has comparable accuracy to GAM- and GLM-based ecological niche models (Ready et al., 2010). It is particularly effective for large areas (e.g., the size of the Adriatic Sea) and when expert knowledge about the species is available at the global scale. Moreover, it is reliable for extracting macro-patterns of climate change influence on species distributions (Coro et al., 2016a).

The AquaMaps *native* algorithm estimates the species niche distribution in its known habitat. It uses a multiplication of environmental parameter envelopes whose ranges are either statistically estimated or defined by an expert. The environmental parameters integrated with the model are 0.5° resolution distributions of depth, salinity, temperature, primary production, distance from land, and sea ice concentration. In the present experiment, the AquaMaps *native* model based on 2019 annual environmental parameters (hereafter referred as *AquaMaps 2019*) was used as a similarity reference for our models.

As a dissimilar reference model, the AquaMaps *native*-2050 model was used (hereafter referred as *AquaMaps 2050*). This model integrates environmental parameters estimated under the Special Report on Emissions Scenario (SRES) *A2* of the Intergovernmental Panel on Climate Change (IPCC). This scenario describes a future world with independent, self-reliant nations with a continuously increasing population. Economic and technological development are assumed to increase non uniformly across the world countries. Of key importance are average surface temperature and salinity that have increasing trends (with localised decreases for salinity), whereas ice concentration decreases globally and water level increases. Our models were checked to be significantly distant from AquaMaps 2050 because this model represents an unlikely scenario for all selected species today. Using the AquaMaps 2050 distributions as unlikely scenarios was particularly consistent for our studied species because their 2050 distributions were significantly different from the AquaMaps *native* distributions (Section 3). The AquaMaps *native* models were downloaded from the AquaMaps website (AquaMaps, 2020; Scarponi et al., 2018), whereas a NetCDF FAIR version of the AquaMaps 2050 model was used, whose consistency and validity was confirmed by other experiments (Coro et al., 2018a). GDAL and CDO software (OSGeo, 2019) was used to downsample the models to 0.1° resolution, through first-order conservative remapping (Schulzweida, 2020), in order to be able to compare them with our models.

2.4.2. Question 2: Can habitat patterns be identified in 2020 with respect to the previous years?

A map comparison procedure was used to answer this question (described in Coro et al. (2014)). This process calculates discrepancy and agreement between two maps. It allows setting a threshold over each probability distribution to conduct presence/absence comparison. Absences are values under the threshold and presences are values over the threshold. The process then uses this classification to calculate discrepancy as the percentage cells where the two distributions disagree. It also calculates Cohen's kappa (Cohen et al., 1960) to estimate agreement with respect to chance. Kappa is classified as poor, slight, fair, moderate, substantial, or excellent according to the Landis and Koch range classifications (Landis and Koch, 1977).

The three FS distributions of each species had different probability ranges. This issue made it difficult to find a common threshold to compare low and high probability cells, which is a common problem when comparing different distributions (Coro et al., 2014; Phillips et al., 2006b). MaxEnt suggested potential habitat suitability thresholds out of a training session over the 2015–2018 data, using a sensitivity-specificity analysis that considered only the observations and environmental data in 2015–2018. However, after this training session, the MaxEnt model was projected onto the 2019 and 2020 data without retraining, and this operation normally produces distributions with new probability ranges (Coro and Bove, 2022; Phillips et al., 2006b). One approach to accommodate for this issue is to allow MaxEnt to extend estimates beyond the parameter ranges observed on the training set (i.e., to disable the model's *clamping* option). However, this technique should be used with caution because it could generate inconsistent results or unnatural projections (Elith et al., 2011). Moreover, the approach assumes that the projection conditions represent a completely different environmental scenario (e.g., in the far past or future). In contrast, our projection scenarios fell within the *clamped* ranges for most variables (Section 3.3). We also experimentally verified that clamping was not useful in overcoming this issue with the data at hand.

Thus, the thresholds suggested by the sensitivity-specificity analysis over the 2015–2018 data could not be used for the 2019 and 2020 distributions. Therefore, conducting a fair comparison between the MaxEnt distributions required setting appropriate thresholds for habitat suitability/unsuitability on each distribution separately; to transform a numerical comparison into a consistent classification comparison. In this case, one possible threshold to use is the first-quartile probability value, as also suggested by O'Brien (1980) and Theil (1982). This property comes out of the observation that although the distribution ranges and shapes can differ between the models, one comparable measure of MaxEnt probability abundance (and thus of habitat suitability extent) is the number of elements with MaxEnt output value over the first quartile. Therefore, we used the first-quartile probability value of each FS distribution to identify areas of low and high suitability. Our results demonstrate that this approach generated comparable FS distributions (Section 3). As for AquaMaps, the log-linear nature of this model allows setting a 0.2 probability value as the threshold (Coro et al., 2013a, 2016a).

Since discrepancy and agreement calculation does not indicate if one distribution corresponds to more suitable habitat than the other, a new

metric was introduced for this scope. In particular, a *suitability score* was defined on the discrepancy cells:

$$S = \frac{\sum_i P'_H(i) - \sum_i P''_H(i)}{N}$$

where i refers to cells on which the two dichotomic P' and P'' distributions differ; N is the total number of cells involved in the comparison; and $P'_H(i)$ and $P''_H(i)$ are the compared habitat distributions using new thresholds that identify *very high* probability zones. These thresholds were set to the 3rd quartiles of the FS distributions and to 0.8 for AquaMaps. The rationale behind the suitability score calculation is that if one distribution indicates very high suitability in the discrepancy areas more often than the other, that distribution is overall more favourable. Thus, $S > 0$ indicates that the first distribution is more suitable than the second (habitat *gain*) - and vice-versa when $S < 0$ (habitat *loss*) - whereas $S = 0$ indicates overall equal suitability between the two distributions (*stable* habitat).

Discrepancy, agreement, and suitability scores over the years can identify habitat change. Increasing habitat suitability from 2015 to 2018 to 2019 and 2020 may indicate overall habitat expansion (*gain*) in 2020, stable suitability may indicate unchanged habitat, and inconstant habitat gain and loss over the years can be associated with potential habitat change.

2.4.3. Question 3: Which parameters drove habitat change in 2020?

MaxEnt also produces single-parameter distributions by training the model with one parameter at-a-time. These parameter distributions allow inferring the parameter ranges that correspond to higher suitability. The inference is straightforward when the involved parameters are independent or bring a high contribution (Coro et al., 2013a, 2015b, 2018c). Our approach enhances parameter independence by re-training MaxEnt after removing low-contributing parameters. Intersecting environmental parameter trends with MaxEnt single-parameter distributions identifies the key responsible parameters for habitat change.

2.4.4. Question 4: Do environmental parameter changes in 2020 depend on the COVID-19 pandemic or also on climate change?

The change in key parameters for our selected species' habitat change could be due to statistical inter-annual fluctuations, or to general global-scale changes such as climate change or the reduction of anthropogenic pressure due to the COVID-19 pandemic. The key factors were investigated by searching for other studies that specifically analysed these parameters in other locations and correlated their trends to climate change or the pandemic. This analysis, combined with the results from the previous evaluation phases, clarified the correlation between anthropogenic pressure on ecosystems due to the COVID-19 pandemic, the coupling with climate change, and potential species habitat change.

2.5. Complete workflow

The complete workflow can be summarised as the production and comparison of MaxEnt distributions of eight selected Adriatic Sea species out of OBIS species observations and Argo data. Each step of the workflow has code and data associated in the open-source repository linked to this paper (see Supplementary Material). The steps can be summarised through the following *phases*:

2.5.1. Phase 1

Retrieve Argo data for the Adriatic and aggregate them at 0.1° spatial resolution (from https://dataselection.euro-argo.eu/). Select probes across years that have a mutual distance under 0.5°. Produce surface, bottom, and water-column average values for each environmental parameter in every reference time frame, i.e., 2015–2018, 2019, and 2020. This phase generated 9 datasets (3 aggregations by 3 years) for Argo parameters (4 in total), i.e., 36 datasets overall. All processing R code and results of this phase are available in the repository linked in the Supplementary Material, within the "Phase 1 - Argo Data Preparation" folder.

2.5.2. Phase 2

Interpolate the 36 environmental parameter datasets through DIVA, using data on ocean current speed components and depth, to obtain uniform 0.1° distributions for the entire Adriatic. Prepare the data as ASC files for MaxEnt. The used DIVA notebook and the results of this phase are available in the repository linked in the Supplementary Material, within the "Phase 2 - Environmental Parameter Distributions" folder.

2.5.3. Phase 3

Retrieve species occurrence records from OBIS (https://obis.org/manual/access/) and prepare them for MaxEnt. For each species, use 2015–2018 OBIS species occurrence records and environmental datasets (plus depth from GEBCO) within a MaxEnt model to produce 8 floating-sensor-based *full-variable* models for 2015–2018 at 0.1° resolution. The retrieved and pre-processed OBIS occurrences, the data preparation scripts, the link to the MaxEnt software, and the MaxEnt results are available in the repository linked in the Supplementary Material, within the "Phase 3 - Occurrence Records and First MaxEnt Run" folder.

2.5.4. Phase 4

Execute MaxEnt again, for each species, using only the parameters that had the highest *percent contribution*, i.e., those within 95% relative difference from the maximum. This phase produced 8 final FS 2015–2018 models, one for each species. It also modelled each species with an optimal selection of parameters associated with their preferred depth ranges. For example, it selected depth and bottom-level parameters for deep-water and benthic species (Section 3.3). As a further step, project the MaxEnt models over the 2019 and 2020 parameter data to obtain FS 2019 and FS 2020 models for the 8 species. The MaxEnt re-execution results are available in the repository linked in the Supplementary Material, within the "Phase 4 - MaxEnt Re-application" folder.

2.5.5. Phase 5

Retrieve AquaMaps 2019 and 2050 distributions and downsample them to 0.1° for consistent comparison with the MaxEnt distributions. The retrieved AquaMaps distributions are available as ESRI-grid files in the repository linked in the Supplementary Material, within the "Phase 5 - AquaMaps Distributions" folder.

2.5.6. Phase 6

Extract parameter quantiles to study trends over the years. Compare MaxEnt distributions to quantify discrepancy and estimate habitat change (though suitability score). The results and the used scripts are available in the repository linked in the Supplementary Material, within the "Phase 6 - Estimate Quantiles" folder.

2.5.7. Phase 7

Identify patterns of habitat change (gain, loss, stability). The extracted patterns are available in the repository linked in the Supplementary Material, within the "Phase 7 - Patterns" folder.

2.5.8. Phase 8

Study the main parameter trends to identify those that influenced habitat change. Understand the relation between these trends and climate change and COVID-19 pandemic (Sections 3.3–3.4).

3. Results

Our method produced distribution maps for 2015–2018, 2019, and 2020 for each of the eight analysed species (Fig. 2). Referring to our evaluation questions (Section 2.4), Section 3.1 addresses question 1;

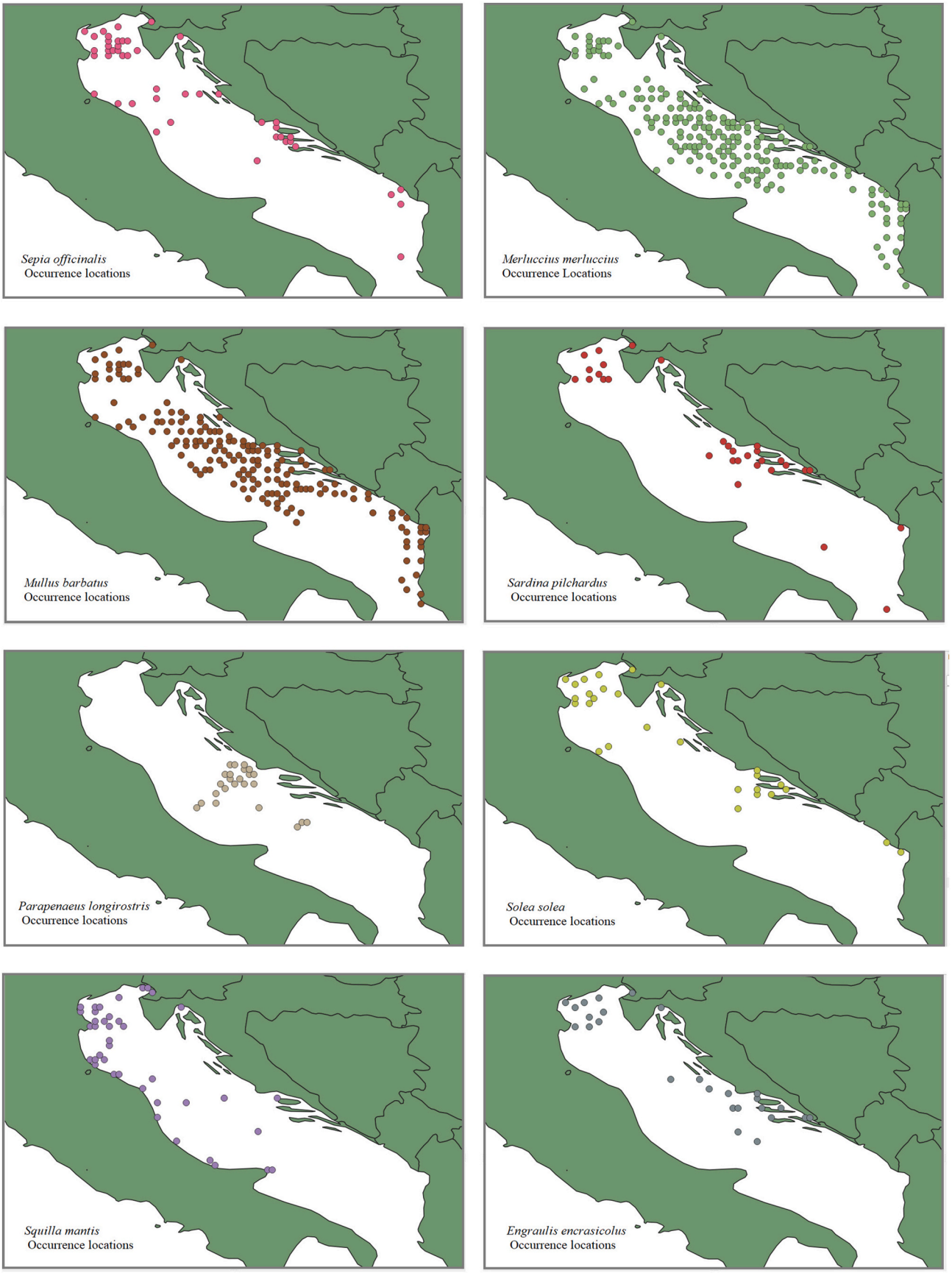

Fig. 1. Distribution of the analysed species' occurrence records, used for our floating sensor based ecological niche models.

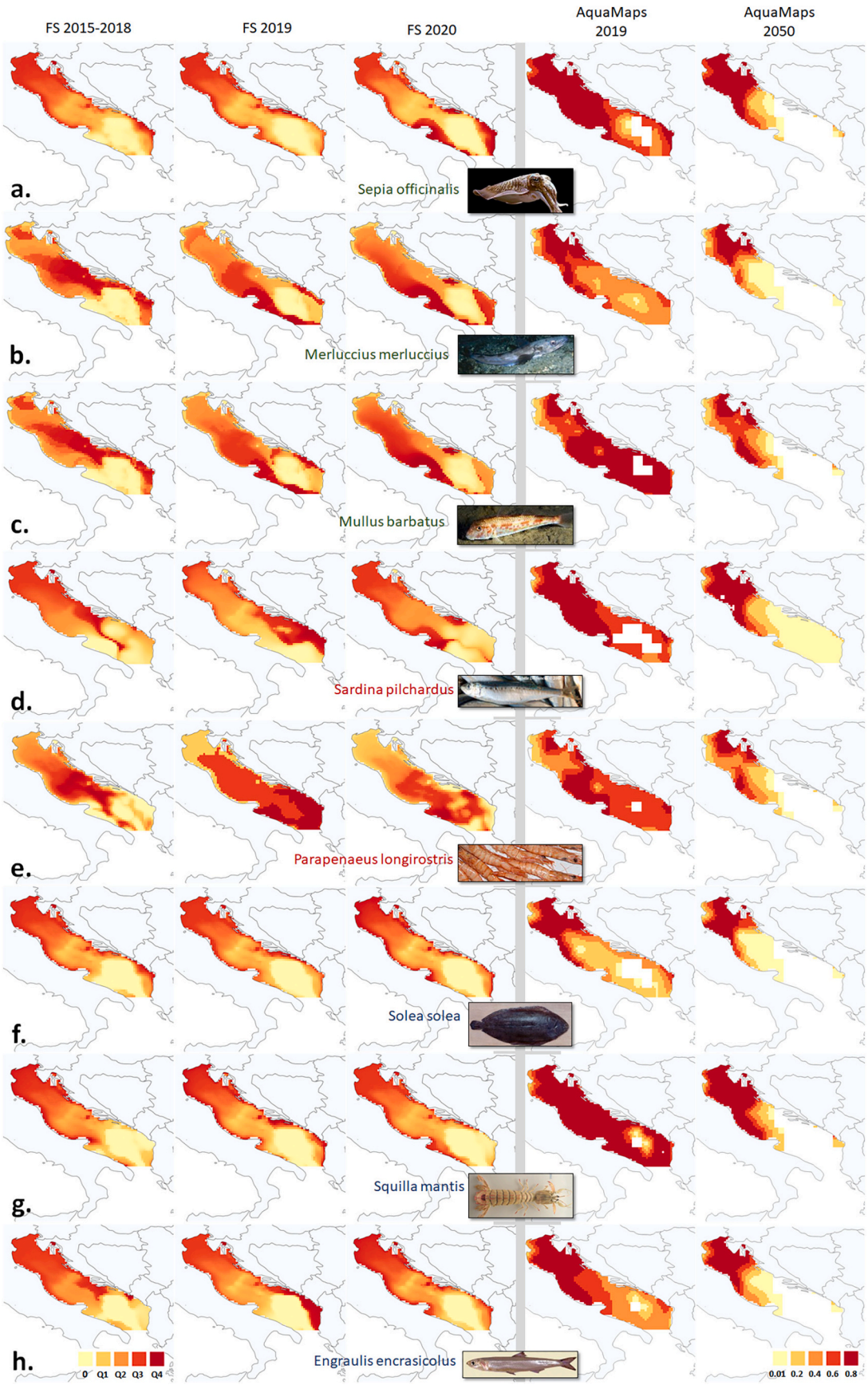

Fig. 2. Ecological niches estimated by our floating sensor based (FS) models for 2015–2018, 2019, and 2020, and AquaMaps 2019 and 2050 over the eight analysed species. Coloured species names indicate habitat gain (green), change (red), or stability (blue) in 2020 with respect to 2015–2018. (For interpretation of the references to colour in this figure legend, the reader is referred to the web version of this article.)

Section 3.2 addresses question 2; Section 3.3 addresses question 3; and Section 3.4 addresses question 4.

For the present experiment, our workflow processed overall 2,166,025 in situ observations for 2015–2018, 364,219 observations for 2019, and 463,352 observations for 2020. These observations covered from ~600 (for chlorophyll-a and DOX) to ~2100 (for temperature and salinity) 0.1° cells in the Adriatic Sea. OBIS occurrence records that had undergone expert review were extracted for these cells to increase observation reliability (at the expense of their quantity). The extracted records between 2015 and 2018 were 47 for *S. officinalis*, 189 for *M. merluccius*, 166 for *M. barbatus*, 39 for *S. pilchardus*, 30 for *P. longirostris*, 28 for *S. solea*, 40 for *S. mantis*, and 27 for *E. encrasicolus*. These observations were distributed across the species' Adriatic habitats (Fig. 1). Although they were theoretically unsuitable for building a detailed model, they were useful for a macroscopic pattern-change analysis of species distributions, in agreement with other ENM approaches that use even a lower number of observations to trace viable environmental envelopes for pattern analyses (Coro et al., 2016a; Kaschner et al., 2006; Kaschner et al., 2011; Ready et al., 2010; Rees, 2008).

3.1. Model consistency

3.1.1. Variable selection and model optimisation

Our feature selection criterion was evaluated using the Kuenm R package (Cobos et al., 2019), which also allowed us to fine-tune the models. This software exhaustively tests the performance of MaxEnt with multiple sets of environmental parameters and finds the optimal configuration of (i) the analytical form of h - among linear, quadratic, product, threshold, hinge, and their combinations (*feature classes*) - and (ii) a penalty factor on the β vector (*regularisation multiplier*) (Merow et al., 2013; Morales et al., 2017). Kuenm allows selecting the optimal model based on the highest Akaike Information Criterion value (AIC) calculated on a test set. To select the optimal parametrisations of our 2015–2018 models, several sets of environmental variables were prepared and evaluated in two ways: (i) on the entire training set (self-performance) and (ii) based on the average AIC over ten randomly extracted observation sets, with an 80–20% training-test set ratio for each extraction and considering only models with omission rate below 5%. The prepared sets of environmental variables included the entire set, the 95% *percent contribution*-based set (Section 2.3), and ten randomly chosen subsets.

The Kuenm evaluation estimated that the optimal regularisation multipliers for all analysed species ranged around 1. Thus, this parameter was fixed to 1 for all models for simplicity, i.e. no penalty was set on β. Moreover, both self-performance and 80–20% validation indicated that the optimal set of environmental variables was the one obtained using a 95% threshold *percent contribution* from the maximum contribution. Finally, using a complex h function that combined all feature classes was optimal for 80–20% validation and also gained high self-accuracy performance. The average AIC over all tests was ~990, whereas the average optimal models' AIC was ~860. These results likely derive from the fact that our selection criterion discards the predictor variables that bring poor and potentially confounding information to the model. Moreover, using complex feature classes reduced the over-fitting bias (Section 2.3) and thus likely increased validation performance.

As a further evaluation step, the *Receiver Operating Characteristic* (ROC) curve was traced for each optimal model to conduct a sensitivity analysis. This analysis calculated the true-positive rate and the false-positive rate using various decision-thresholds on the model output. Consequently, all optimal models were verified to achieve an *Area Under the Curve* (AUC) (i.e., the integral of the ROC curve) over 0.95. Specifically, AUC was averagely 0.96 [0.954;0.97] for the optimal models, and 0.83 [0.78;0.95] for sub-optimal models. This property guaranteed that the probability distributions simulated by each model were significantly higher on species-presence locations than on random locations. All these quality checks aimed to optimise model robustness in a context of scattered environmental data and few observation data.

It is worth noting that using AIC as a selection criterion can be prone to criticisms, especially because AIC tends to select models with a higher number of parameters among equal-likelihood models (Arnold, 2010; Guthery et al., 2005). However, issues especially arise if AIC were used (i) as the only selection criterion, (ii) without adding prior information to guide selection, and (iii) to build models that pretend to assess ecological reality (Reside et al., 2019; Roy-Dufresne et al., 2019; Zhang et al., 2018). Therefore, our use of AIS, through Kuenm, can be tolerated because we (i) did not assume the optimal models to be punctually reliable, but generally reliable to assess macroscopic changes when compared to each other, (ii) used a prior condition to evaluate only the models with omission rates below 5%, (iii) forcibly introduced a further parametrisation that involved the 95% percent contribution-based set; (iv) added sensitivity analysis to assess model validity further; (v) checked model consistency through comparison with AquaMaps; (vi) introduced constraints to avoid over-fitting. Indeed, the optimal models did not use the highest number of environmental parameters and complex regularisation and penalty conditions.

The optimal parametrisations estimated for the FS 2015–2018 models were also used for the FS 2019 and FS 2020 projections. The resulting optimal distributions are reported in Fig. 2.

3.1.2. Comparison with AquaMaps

The dissimilarity between our maps and AquaMaps 2019 was reasonably low, i.e., averaging below 20% (19.14%, Table 1). Furthermore, a *fair* kappa agreement (according to Landis and Koch classification, Landis and Koch (1977)) occurred for 81.3% of the comparisons. The greatest discrepancy, corresponding to *slight* agreement, was found for *E. encrasicolus* and *M. merluccius*. For these species (Figs. 2-h and -b), AquaMap 2019 extended more into south Adriatic. As for AquaMaps 2050, the IPCC SRES A2 scenario was found to be significantly distant from our distributions, with a ~30% average discrepancy and *poor/marginal* agreement with 87.5% of the distributions. The highest similarity - with *moderate* kappa agreement - occurred for *S. mantis* (19.2% discrepancy vs FS 2015–2018, 17.57% vs FS 2019, and 19.07% vs FS 2020). The FS models indicated that this species had a stable habitat concentrated in northern Adriatic, whereas AquaMaps 2019 estimated a possible presence in south Adriatic. Notably, OBIS does not report expert-verified occurrences of *S. mantis* in south Adriatic, which enforces the consistency of our model.

Overall, this assessment indicates that our distributions generally agreed with an independent reference model (AquaMaps 2019) and were far from an unlikely scenario (AquaMaps 2050). Thus, despite the poor data, the predictions of our models were not poor, which permitted us to conduct further analyses and extract general patterns over the Adriatic.

3.2. Habitat change classification

Based on the discrepancy (Table 1) and the suitability score (Table 2) calculations, detailed habitat gain and loss trends were traced per species. In particular, *S. officinalis* habitat expanded in 2020 with respect to both 2015–2018 (+3.95%) and 2019 (+0.14%) with significant discrepancy (12.36% vs. 2015–2018 and 7.18% vs. 2019) (Fig. 2-a). Distributional differences were found off the Apulian coasts and in the south Balkans. The FS 2020 distribution was also similar to AquaMaps 2019, with *substantial* kappa agreement, because both the distributions indicated extension towards south-east and south-west. In northern Adriatic, the FS 2020 map presented a similar distribution to the other FS maps, with *substantial* kappa agreement. This distribution was different from AquaMaps 2050 (24.72% discrepancy), which predicted habitat loss throughout south Adriatic. Overall, this analysis indicates habitat gain for this species in 2020.

M. merluccius habitat expanded in 2020 with respect to 2015–2018

Table 1
Discrepancy between the ecological niche models of the eight species involved in our experiment. Model names refer to floating sensor models for 2015–2018 (FS 2015–2018), 2019 (FS 2019), 2020 (FS 2020), and AquaMaps 2019 and 2050. Coloured numbers refer to Cohen's kappa values corresponding to at-least-moderate (green), slight (orange), or poor agreement (red) according to Landis & Koch interpretation. Bold-highlighted text indicates the most similar distribution for each model. Coloured species names indicate habitat gain (green), change (red), or stability (blue) in 2020 with respect to 2015–2018.

Sepia officinalis

	FS 2015-2018	FS 2019	FS 2020	AquaMaps 2019	AquaMaps 2050
FS 2015-2018	-	**10.06%**	12.36%	15.24%	21.71%
FS 2019	10.06%	-	**7.18%**	15.50%	22.71%
FS 2020	12.36%	**7.18%**	-	14.87%	24.72%
AquaMaps 2019	15.24%	15.50%	**14.87%**	-	43.14%
AquaMaps 2050	**21.71%**	22.71%	24.72%	43.14%	-

Merluccius merluccius

	FS 2015-2018	FS 2019	FS 2020	AquaMaps 2019	AquaMaps 2050
FS 2015-2018	-	**18.53%**	17.82%	25.92%	34.25%
FS 2019	18.53%	-	**5.89%**	22.61%	40.90%
FS 2020	17.82%	**5.89%**	-	22.47%	41.03%
AquaMaps 2019	25.92%	22.61%	**22.47%**	-	52.26%
AquaMaps 2050	**34.25%**	40.90%	41.03%	52.26%	-

Mullus barbatus

	FS 2015-2018	FS 2019	FS 2020	AquaMaps 2019	AquaMaps 2050
FS 2015-2018	-	18.53%	**16.24%**	22.61%	24.28%
FS 2019	18.53%	-	**9.20%**	18.88%	30.43%
FS 2020	16.24%	**9.20%**	-	19.60%	27.42%
AquaMaps 2019	22.61%	**18.88%**	19.60%	-	38.25%
AquaMaps 2050	**24.28%**	30.43%	27.42%	38.25%	-

Sardina pilchardus

	FS 2015-2018	FS 2019	FS 2020	AquaMaps 2019	AquaMaps 2050
FS 2015-2018	-	**14.51%**	22.84%	16.69%	21.64%
FS 2019	**14.51%**	-	29.60%	24.22%	29.17%
FS 2020	22.84%	29.60%	-	**18.32%**	20.89%
AquaMaps 2019	**16.69%**	24.22%	18.32%	-	32.69%
AquaMaps 2050	21.64%	29.17%	**20.89%**	32.69%	-

Parapenaeus longirostris

	FS 2015-2018	FS 2019	FS 2020	AquaMaps 2019	AquaMaps 2050
FS 2015-2018	-	47.13%	34.34%	**21.71%**	26.35%
FS 2019	47.13%	-	**20.83%**	21.83%	58.85%
FS 2020	34.34%	20.83%	-	**20.70%**	41.91%
AquaMaps 2019	21.71%	21.83%	**20.70%**	-	47.88%
AquaMaps 2050	**26.35%**	58.85%	41.91%	47.88%	-

Solea solea

	FS 2015-2018	FS 2019	FS 2020	AquaMaps 2019	AquaMaps 2050
FS 2015-2018	-	**6.18%**	6.75%	11.23%	34.63%
FS 2019	6.18%	-	**2.73%**	11.23%	34.63%
FS 2020	6.75%	**2.73%**	-	10.85%	34.63%
AquaMaps 2019	11.23%	11.23%	**10.85%**	-	52.46%
AquaMaps 2050	**34.63%**	**34.63%**	**34.63%**	52.46%	-

Squilla mantis

	FS 2015-2018	FS 2019	FS 2020	AquaMaps 2019	AquaMaps 2050
FS 2015-2018	-	12.07%	**4.74%**	19.70%	19.20%
FS 2019	12.07%	-	**10.63%**	19.70%	17.57%
FS 2020	**4.74%**	10.63%	-	19.70%	19.07%
AquaMaps 2019	**19.70%**	**19.70%**	**19.70%**	-	41.87%
AquaMaps 2050	19.20%	**17.57%**	19.07%	41.87%	-

Engraulis encrasicolus

	FS 2015-2018	FS 2019	FS 2020	AquaMaps 2019	AquaMaps 2050
FS 2015-2018	-	12.79%	**12.07%**	21.90%	30.80%
FS 2019	12.79%	-	**4.45%**	21.90%	30.80%
FS 2020	12.07%	**4.45%**	-	21.90%	30.65%
AquaMaps 2019	**21.90%**	**21.90%**	**21.90%**	-	53.00%
AquaMaps 2050	30.80%	30.80%	**30.65%**	53.00%	-

Table 2
Suitability score comparison between the ecological niche models of the eight species involved in our experiment. Model names indicate floating sensor models for 2015–2018 (FS 2015–2018), 2019 (FS 2019), 2020 (FS 2020), and AquaMaps 2019 and 2050. Scores are reported only for the FS models to ease the reading. Coloured numbers highlight habitat gain (green), loss (red), or stability (blue) in 2020. Coloured species names indicate habitat gain (green), change (red), or stability (blue) in 2020 with respect to 2015–2018.

Sepia officinalis

	FS 2015-2018	FS 2019	FS 2020	AquaMaps 2019	AquaMaps 2050
FS 2015-2018	-	Loss (-0.29%)	Loss (-3.95%)	Loss	Gain
FS 2019	Gain (+0.29%)	-	Loss (-0.14%)	Loss	Gain
FS 2020	Gain (+3.95%)	Gain (+0.14%)	-	Loss	Gain
AquaMaps 2019	Gain	Gain	Gain	-	Gain
AquaMaps 2050	Loss	Loss	Loss	Loss	-

Merluccius merluccius

	FS 2015-2018	FS 2019	FS 2020	AquaMaps 2019	AquaMaps 2050
FS 2015-2018	-	Loss (-7.04%)	Loss (-5.68%)	Loss	Gain
FS 2019	Gain (+7.04%)	-	Gain (+0.36%)	Loss	Gain
FS 2020	Gain (+5.68%)	Loss (-0.36%)	-	Loss	Gain
AquaMaps 2019	Gain	Gain	Gain	-	Stable
AquaMaps 2050	Loss	Loss	Loss	Stable	-

Mullus barbatus

	FS 2015-2018	FS 2019	FS 2020	AquaMaps 2019	AquaMaps 2050
FS 2015-2018	-	Loss (-7.61%)	Loss (-3.38%)	Loss	Gain
FS 2019	Gain (+7.61%)	-	Gain (+1.94%)	Loss	Gain
FS 2020	Gain (+3.38%)	Loss (-1.94%)	-	Loss	Gain
AquaMaps 2019	Gain	Gain	Gain	-	Gain
AquaMaps 2050	Loss	Loss	Loss	Loss	-

Sardina pilchardus

	FS 2015-2018	FS 2019	FS 2020	AquaMaps 2019	AquaMaps 2050
FS 2015-2018	-	Loss (-4.31%)	Loss (-4.6%)	Loss	Gain
FS 2019	Gain (+4.31%)	-	Gain (+5.46%)	Gain	Gain
FS 2020	Gain (+4.6%)	Loss (-5.46%)	-	Gain	Gain
AquaMaps 2019	Gain	Loss	Loss	-	Gain
AquaMaps 2050	Loss	Loss	Loss	Loss	-

Parapenaeus longirostris

	FS 2015-2018	FS 2019	FS 2020	AquaMaps 2019	AquaMaps 2050
FS 2015-2018	-	Loss (-14.87%)	Loss (-8.33%)	Loss	Gain
FS 2019	Gain (+14.87%)	-	Gain (+7.04%)	Loss	Gain
FS 2020	Gain (+8.33%)	Loss (-7.04%)	-	Loss	Gain
AquaMaps 2019	Gain	Gain	Gain	-	Gain
AquaMaps 2050	Loss	Loss	Loss	Loss	-

Solea solea

	FS 2015-2018	FS 2019	FS 2020	AquaMaps 2019	AquaMaps 2050
FS 2015-2018	-	Stable	Loss (-0.5%)	Gain	Gain
FS 2019	Stable	-	Stable	Gain	Gain
FS 2020	Gain (+0.5%)	Stable	-	Gain	Gain
AquaMaps 2019	Loss	Loss	Loss	-	Gain
AquaMaps 2050	Loss	Loss	Loss	Loss	-

Squilla mantis

	FS 2015-2018	FS 2019	FS 2020	AquaMaps 2019	AquaMaps 2050
FS 2015-2018	-	Loss (-1.22%)	Loss (-0.36%)	Loss	Gain
FS 2019	Gain (+1.22%)	-	Gain (+0.72%)	Loss	Gain
FS 2020	Gain (+0.36%)	Loss (-0.72%)	-	Loss	Gain
AquaMaps 2019	Gain	Gain	Gain	-	Gain
AquaMaps 2050	Loss	Loss	Loss	Loss	-

Engraulis encrasicolus

	FS 2015-2018	FS 2019	FS 2020	AquaMaps 2019	AquaMaps 2050
FS 2015-2018	-	Loss (-5.6%)	Stable	Gain	Gain
FS 2019	Gain (+5.6%)	-	Gain (+1.15%)	Stable	Gain
FS 2020	Stable	Loss (-1.15%)	-	Gain	Gain
AquaMaps 2019	Loss	Stable	Loss	-	Stable
AquaMaps 2050	Loss	Loss	Loss	Stable	-

(+5.68%) but minimally lost habitat with respect to 2019 (−0.36%) (Fig. 2-b). The discrepancy vs 2019 (5.89%) was lower than vs 2015–2018 (17.82%). The similarity between FS 2020 and FS 2019 was due to minimal differences in the south-eastern Adriatic. Furthermore, FS 2019 reported habitat gain (+7.04%) against FS 2015–2018, which indicated an increasing habitat extension trend over the years. The greatest discrepancy between FS 2020 and AquaMaps 2019 was in the south Adriatic, where AquaMaps reported high suitability. The FS 2020 distribution was also different from AquaMaps 2050 (41.03% discrepancy) due to the AquaMaps-predicted habitat loss throughout south Adriatic in 2050. Overall, this analysis suggests habitat *gain* for this species in 2020 because its habitat substantially expanded with respect to 2015–2018 and was similar to a habitat-favourable 2019.

Similarly, *M. barbatus* habitat expanded in 2020 with respect to 2015–2018 (+3.38%) and slightly lost habitat with respect to 2019 (−1.94%) (Fig. 2-c). The discrepancy vs 2019 (9.20%) was lower than vs 2015–2018 (16.24%). The similarity between FS 2020 and FS 2019 was due to minimal differences in middle Adriatic. Furthermore, FS 2019 resulted in habitat gain (+7.61%) against FS 2015–2018, which indicated an increasing habitat extension trend over the years. The FS 2020 was also similar to AquaMaps 2019 (19.6% discrepancy and *moderate* agreement) because both models reported high suitability for south Adriatic. For this reason, FS 2020 was different from AquaMaps 2050 (27.42% discrepancy and *poor* agreement), which foresaw habitat loss in south Adriatic. Overall, this analysis indicates habitat *gain* for *M. barbatus* in 2020 because its habitat substantially expanded with respect to 2015–2018 and was similar to an advantageous 2019.

S. pilchardus habitat expanded with respect to 2015–2018 (+4.6%) but substantially lost habitat with respect to 2019 (−5.46%) (Fig. 2-d). The discrepancy between FS 2020 and FS 2019 (29.6%) was concentrated off Apulian coasts (with gain in 2020) and in the Balkans (with gain in 2019). Furthermore, FS 2019 reported habitat gain (+4.31%) vs 2015–2018 especially in south-western Adriatic and off central Italian coasts. Thus, habitat trend was not stable, and the FS 2020 habitat suitability patterns changed with respect to FS 2015–2018 and FS 2019. Due to the high suitability reported in south Adriatic, all FS distributions had *moderate* agreement with AquaMaps 2019. The discrepancy between FS 2020 and AquaMaps 2050 (20.89%) was lower than the one of the previous species because also AquaMaps 2050 foresaw suitable habitat in 2050 in south Adriatic. Overall, this analysis indicates habitat *change* for *S. pilchardus* in 2020 because no definite trend and pattern was present across the models.

Similarly, *P. longirostris* habitat expanded with respect to 2015–2018 (+8.33%) but substantially lost habitat with respect to 2019 (−7.04%) (Fig. 2-e). The discrepancy between FS 2020 and FS 2019 (20.83%) was concentrated in the south and middle Adriatic (with gain in 2019). In the same areas, FS 2019 reported substantial habitat gain (+14.87%) vs 2015–2018. Thus, habitat trend was unstable since the FS 2020 habitat suitability patterns were substantially different with respect to FS 2015–2018 and FS 2019. All FS distributions had *moderate* kappa agreement with AquaMaps 2019 due to the high habitat suitability AquaMaps indicated in south Adriatic. In contrast, since AquaMaps 2050 indicated great habitat loss in south Adriatic, the discrepancy with FS distributions was large (42.37% average). Overall, this analysis indicates habitat *change* for *P. longirostris* in 2020 because no definite trend and pattern was present across the models.

S. solea slightly gained habitat with respect to 2015–2018 (+0.5%) and presented stable habitat suitability with respect to 2019 (Fig. 2-f). The discrepancy between FS 2020 and FS 2015–2018 (6.75%) was due to a slightly higher suitability area off Apulian coasts by FS 2020. The habitat change trend was thus stable, and the similarity and the kappa agreement between the FS 2020 and the other distribution was *substantial*. The FS distributions also had *substantial* kappa agreement with AquaMaps 2019, with very similar patterns throughout the Adriatic. Since AquaMaps 2050 foresaw great habitat loss in south Adriatic (except for a small area in southern Balkans), its discrepancy with respect to the FS distributions was high (34.63%). Overall, this analysis indicates *stable* habitat for *S. solea* from 2015 to 2018 to 2020.

S. mantis slightly gained habitat with respect to 2015–2018 (+0.36%) and slightly lost habitat with respect to 2019 (−0.72%) (Fig. 2-g). The discrepancy between FS 2020 and the other FS distributions was concentrated off the Apulian coasts. The habitat change trend was overall stable, and kappa agreement between the FS 2020 and the other distribution was *substantial*. The FS distributions also had *moderate* kappa agreement with AquaMaps 2019, which reported habitat suitability for most of the Adriatic. Since AquaMaps 2050 reported high probability areas in northern and middle Adriatic and off northern Albanian coasts, kappa agreement with the FS maps was *moderate*. Overall, *S. solea* presented an overall *stable* habitat from 2015 to 2018 to 2020.

E. encrasicolus presented stable habitat distribution with respect to 2015–2018 and a slight suitability loss with respect to 2019 (−1.15%) (Fig. 2-h). The discrepancy between FS 2020 and FS 2019 was due to a higher probability area off Albanian coasts. The habitat change trend was overall stable, and the mutual similarity had *substantial* kappa agreement. The FS distributions also had *moderate* kappa agreement with AquaMaps 2019, which presented a decreasing gradient from north to south. Since AquaMaps 2050 reported habitat loss for middle and south Adriatic, kappa agreement with the FS maps was *poor*. Overall, *E. encrasicolus* presented an approximately *stable* habitat from 2015 to 2018 to 2020.

3.3. Habitat change due to environmental parameter change

The key driving parameters for habitat change in 2020 were identified through the analysis of their *percent contributions* (Table 4). Notably, the MaxEnt parameter selection corresponded to known environmental preferences of the studies species. For example, *M. barbatus* lives in sandy, muddy bottoms near river mouths (Esposito et al., 2014), and indeed its key parameters were bottom temperature and depth, but also chlorophyll-a and DOX averages in the upper water column. *S. pilchardus* habitat-depth ranges between 10 and 100 m (Santos et al., 2006), and indeed it was associated with bottom and water-column averaged parameters. *P. longirostris* is a deep-water species, and its habitat was indeed highly dependent on depth. However, its distribution also depends on temperature and DOX in the water column (Ardizzone et al., 1990) as confirmed by our MaxEnt model.

The single-parameter charts of FS 2015–2018 - produced by MaxEnt after training - were used to identify the most significant driving factors of the change (Fig. 3). In addition, parameter quartiles were extracted to understand if variation trends could be identified among the driving factors (Table 3). To enhance readability, only the parameter distributions that were sensitive to parameter change over the years, i.e., with probability density variation over 0.05 - were reported in Fig. 3. Other probability distributions indicated non-significant variation in correspondence of the median parameter change over the years (e.g., they reported a plateau over the variation range), and were omitted. Since this analysis was conducted on the optimal models, only the parameters that showed significant percent contribution were analysed for each species' distribution.

As regards the species that expanded habitat, *S. officinalis* was mainly supported by a general decreasing trend, from 2015 to 2020, of average DOX (with median going from 234.1 to 213.7 $\mu mol/kg$, Table 3) and an increasing trend of bottom temperature over the years (with median rising from 14.15 to 14.32 °C, Table 3). These two parameters significantly contributed to the MaxEnt model, and their trends went towards maxima of the single-parameter densities (Fig. 3-a). Change in the other parameters did not influence habitat gain and thus was not discussed. *M. merluccius* and *M. barbatus* expanded habitat especially because of increasing bottom temperature trend and decreasing average chlorophyll-a over time (from 0.039 to 0.034 mg/m^3, Table 3). These changes moved the habitat to higher MaxEnt probability values and

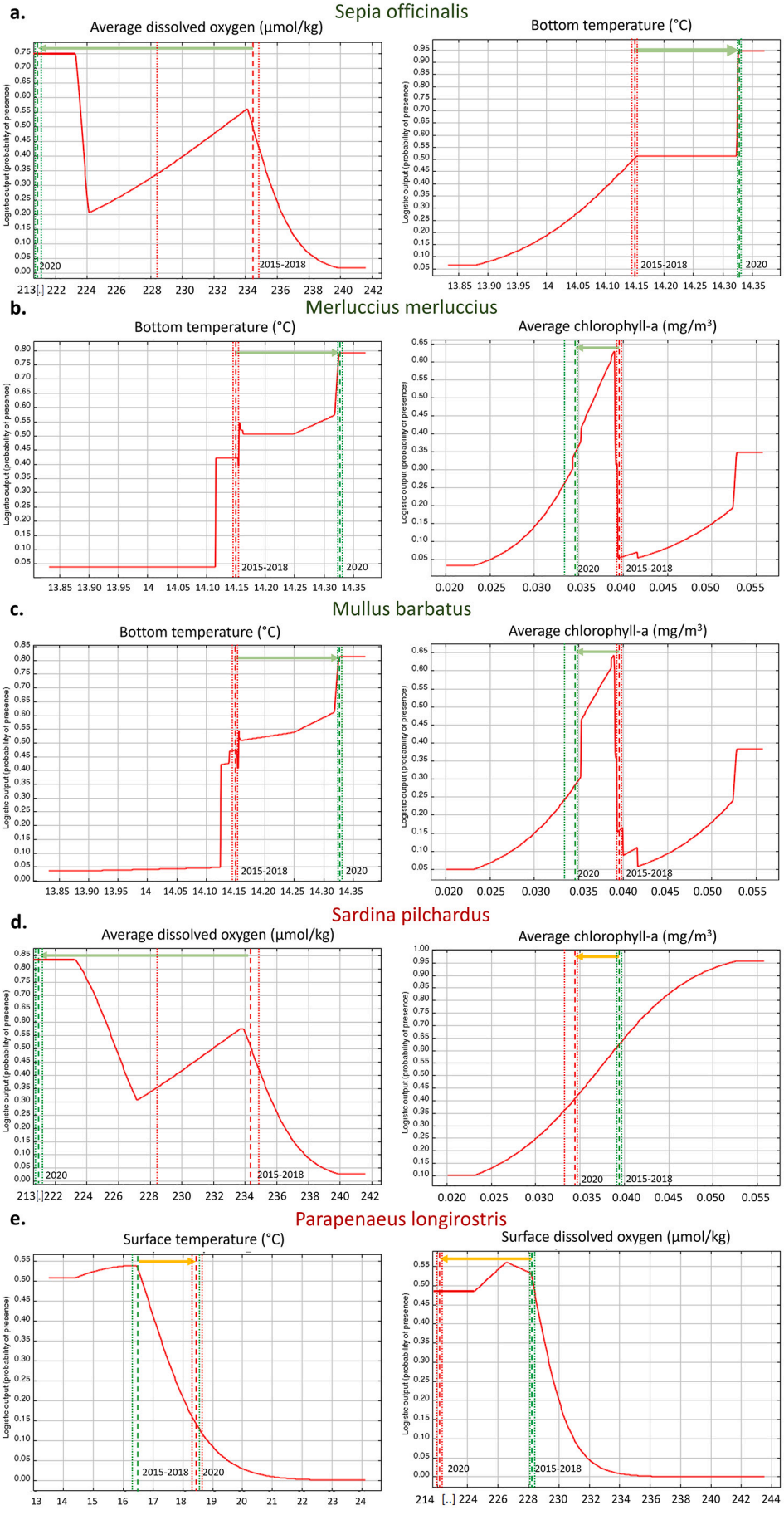

Fig. 3. Single-parameter MaxEnt probability densities across the studied species. Only the charts of the key parameters driving habitat gain and change are reported. Coloured species names in the chart titles indicate those that gained (green) or changed (red) habitat in 2020 with respect to 2015–2018. Vertical bars highlight the values in 2015–2018 and 2020 at the intersection with medians as dashed lines and quartiles 1 and 3 as dotted lines. A green horizontal arrow, from a red to a green vertical line, indicates a general habitat suitability increase from 2015 to 2018 to 2020. Conversely, a yellow horizontal arrow, from a green to a red vertical line, indicates habitat suitability decrease from 2015 to 2018 to 2020. (For interpretation of the references to colour in this figure legend, the reader is referred to the web version of this article.)

consequently increased habitat gain (Figs. 3-b and -c).

As regards the species that changed habitat, the inconstant trend of *S. pilchardus* was due to average DOX and average chlorophyll-a decrease (Table 3). This decrease changed habitat suitability in 2020 with respect to 2015–2018 (Fig. 3-d), and also generated different patterns between the FS 2019 and 2020 distributions. Habitat change for *P. longirostris* was mainly driven by surface temperature modulations (from 16.6 °C in 2015–2018 to 19.7 °C in 2019 and 18.4 °C in 2020, Table 3) and surface DOX modulations (from 228.36 *μmol/kg* in 2015–2018 to 227.8 *μmol/kg* in 2019 and 214.7 *μmol/kg* in 2020, Table 3). For this species, this parameter combination resulted in a less favourable habitat in 2020 than the previous years (Fig. 3-e).

The species with stable habitat distributions presented a robust response to environmental change, and no parameter could be highlighted over the others.

3.4. Environmental parameter relation with climate change and COVID-19 pandemic

The parameters that principally drove distribution changes - i.e., temperature, chlorophyll-a, and DOX - were analysed to understand if their change depended on inter-annual climatic variations, general climate change trends or the COVID-19 pandemic (Table 5).

The general change of temperature positively affected the distributions of *S. officinalis*, *M. merluccius*, *M. barbatus*, but negatively the one of *P. longirostris*. Despite the cooling effect of La Niña since August 2020 - which mainly affected surface temperature - global temperature increased up to 1.2 °C above pre-industrial value (DownToEarth, n.d.;

Table 3
Median, 1st and 3rd quartiles of the environmental parameter distributions used in our experiment over the Adriatic Sea, estimated from Argo data. *Average* aggregation type indicates parameter average over the entire water column.

Parameter name	Aggregation type	Years	Median	1st Quartile	3rd Quartile
Temperature (°C)	Average	2015–2018	14.95	14.94	15.02
		2019	14.74	14.74	14.75
		2020	15.26	15.25	15.26
	Bottom	2015–2018	14.15	14.14	14.16
		2019	14.10	14.09	14.10
		2020	14.32	14.31	14.32
	Surface	2015–2018	16.58	16.50	18.48
		2019	19.67	18.51	19.71
		2020	18.40	18.35	18.55
Salinity (PSU)	Average	2015–2018	38.83	38.83	38.83
		2019	38.90	38.90	38.90
		2020	38.97	38.97	38.97
	Bottom	2015–2018	38.82	38.82	38.82
		2019	38.86	38.85	38.86
		2020	38.90	38.89	38.90
	Surface	2015–2018	38.78	38.77	38.78
		2019	38.80	38.80	38.82
		2020	39.01	39.00	39.01
Chlorophyll-a (mg/m^3)	Average	2015–2018	0.0391	0.0389	0.0392
		2019	0.0366	0.0365	0.0377
		2020	0.0343	0.0331	0.0344
	Bottom	2015–2018	0.0051	0.0027	0.0052
		2019	0.0056	0.0056	0.0057
		2020	0.0028	0.0027	0.0029
	Surface	2015–2018	0.0436	0.0432	0.0438
		2019	0.2213	0.2202	0.2222
		2020	0.1896	0.1888	0.1907
Dissolved oxygen (*μmol/kg*)	Average	2015–2018	234.12	228.72	234.26
		2019	220.50	219.88	220.53
		2020	213.70	213.67	213.72
	Bottom	2015–2018	214.32	212.41	214.39
		2019	216.81	216.40	216.84
		2020	210.33	210.16	210.35
	Surface	2015–2018	228.36	228.25	228.64
		2019	227.80	227.66	227.92
		2020	214.73	214.47	214.84

Table 4
Percent contribution and permutation importance of the most habitat-predictive parameters for the 8 analysed species. Bold-highlighted text indicates, for each species, the major drivers of habitat change from 2015 to 2018 to 2020. Coloured species names indicate habitat gain (green), change (red), or stability (blue) in 2020 with respect to 2015–2018.

Species name	Parameter	Percent contribution (%)	Permutation importance (%)
Sepia officinalis	depth	77.6	59.3
	average dissolved oxygen	5.4	8.4
	average salinity	5.3	21.2
	bottom dissolved oxygen	4.9	0
	bottom temperature	4.6	0.1
	bottom salinity	1.4	5.6
	surface chlorophyll-a	0.8	5.5
Merluccius merluccius	**bottom temperature**	48.2	27.6
	average chlorophyll-a	24.6	14.2
	depth	7.8	26.4
	surface chlorophyll-a	6.4	16.5
	average salinity	4.7	5.4
	surface dissolved oxygen	3.9	3
	surface salinity	2.4	1.5
	average temperature	1.9	5.4
Mullus barbatus	**bottom temperature**	49.5	24.7
	average chlorophyll-a	24.7	13.6
	surface dissolved oxygen	6.7	6.8
	depth	6.5	20.1
	bottom chlorophyll-a	5.5	17.4
	surface chlorophyll-a	3.1	10.4
	bottom dissolved oxygen	2.3	3.8
	surface salinity	1.7	3.2
Sardina pilchardus	bottom chlorophyll-a	66.6	54.4
	average dissolved oxygen	16.7	0.5
	average chlorophyll-a	11.9	20
	bottom dissolved oxygen	4.2	0
	depth	0.6	25.1
Parapenaeus longirostris	depth	66.2	45
	surface temperature	12.9	40.4
	average temperature	9.6	14.5
	average dissolved oxygen	8.1	0
	surface dissolved oxygen	3.2	0.1
Solea solea	depth	80.6	84.9
	average temperature	9.7	0
	average dissolved oxygen	5.1	0
	bottom chlorophyll-a	2.8	9.7
	average salinity	1.8	5.4
Squilla mantis	depth	66	77.3
	bottom chlorophyll-a	14.4	6.3
	average temperature	14.1	16.1
	surface temperature	4.1	0.3
	bottom salinity	1.5	0
Engraulis encrasicolus	depth	63	31
	surface dissolved oxygen	20.1	43.6
	bottom chlorophyll-a	5.6	25.4
	bottom dissolved oxygen	5.5	0
	average chlorophyll-a	3.5	0
	average dissolved oxygen	2.4	0

Table 5
Summary of the principal environmental parameters that drove species distribution change in 2020. For each parameter, the table reports (i) the general (increasing/decreasing) trend with respect to the past years, (ii) the main reasons of the change, (iii-iv) the species whose distributions were positively affected (i.e. they increased in 2020) or negatively affected by that parameter change.

Principal parameters that drove selected-species distribution change in 2020	General trend in 2020 wrt past years	Possible reason of the change	Species with positively affected distribution by the change	Species with negatively affected distribution by the change
Temperature	Increasing	Climate change	*Sepia officinalis, Merluccius merluccius, Mullus barbatus*	*Parapenaeus longirostris*
Dissolved Oxygen	Decreasing	Climate change and pollution	*S. officinalis*	*Sardina pilchardus, P. longirostris*
Chlorophyll-a	Decreasing	COVID-19 pandemic	*M. merluccius, M. barbatus*	*S. pilchardus*

United Nations, 2021a; World Meterological Organization, 2021).

Similarly, the general decrease of DOX positively affected the habitat of *S. officinalis*, but negatively the habitats of *S. pilchardus* and *P. longirostris*. Although in 2020 DOX increased in several world areas, as the consequence of the quality improvement of coastal environments during the pandemic (Arif et al., 2020), in the Adriatic Sea the trend has been strongly decreasing in the last two decades (Kralj et al., 2019b). The Adriatic has a generally increasing DOX gradient from north to south consequent to its water circulation, a decreasing nutrient concentration provided by rivers, and a higher phytoplankton development in northern regions (especially in autumn and winter) (Zavatarelli et al., 1998). The overall average DOX decrease trend is probably due to a general DOX depletion at the Adriatic Sea floor. DOX level correlates with plankton respiration and benthic oxygen consumption, which has been exceeding the oxygen produced by microalgae and the one coming from oxygenated water (Kralj et al., 2019b; Lipizer et al., 2014). This condition has been assessed as being a probable consequence of bottom temperature and salinity increase due to climate change (Kralj et al., 2019a; Lipizer et al., 2014; Marasović et al., 2005), and indeed was never observed before 1984 (Justić et al., 1987).

Conversely, the strong chlorophyll-a decrease in 2020 - i.e., −6% in the water column, −50% at the sea bottom, and −14% at the surface than 2019, based on the Argo data (Table 3) - could be correlated with the COVID-19 pandemic. Although this correlation cannot be demonstrated with our data, some supporting conjectures can be reported from other studies. Chlorophyll-a is indeed one of the main indicators of ocean productivity and is an integral part of the carbon cycle and oxygen production. The carbon cycle indeed depends on carbon dioxide consumption during photosynthetic primary production and inorganic carbon production during biomineralisation. The global balance of the natural carbon cycle implies that a large decrease of carbon dioxide (CO_2) in the atmosphere likely corresponds to a lower chlorophyll-a level because of the lower demand for CO_2 uptake (Shehhi and Samad, 2021). In 2020, a 7% reduction in the global carbon dioxide emissions was measured from satellite and in situ estimates due to big industry closure in several world countries with high industrial activity and large population (Le Quéré et al., 2020). As a probable consequence (Adwibowo, 2020; Mishra et al., 2020), a consistent decrease of chlorophyll-a was observed in many areas throughout 2020. For example, a 123 t reduction of CO_2 emission in south China corresponded to a measured 5% reduction of chlorophyll-a during the pandemic (Shehhi and Samad, 2021). This phenomenon was also observed in north Europe, South Korea, south-east United States, the Pacific Ocean, Middle East, western Africa, and south-east Australia. Thus, the chlorophyll-a decrease was probably a global phenomenon correlated with anthropogenic activity reduction (Shehhi and Samad, 2021).

Thus, our analysis indicates that the COVID-19 pandemic likely resulted in modifying three species habitats among those studied: it positively affected the distributions of *M. merluccius* and *M. barbatus*, but negatively the one of *S. pilchardus*.

4. Discussion and conclusions

This paper has presented an analysis of habitat change in 2020 with respect to the previous years (2015–2018 aggregated and 2019), based on floating sensor information and species occurrence records from the OBIS data collection. Our experiment estimated the habitat of 8 commercial species of the Adriatic Sea over this period. The produced ecological niche distributions were sufficiently reliable when compared to those produced by an independent model. They were similar to a model based on 2019 environmental conditions (AquaMaps 2019) and very distant from a model based on a currently improbable environmental scenario (AquaMaps 2050).

Our distributions were suitable for a pattern analysis to investigate if habitat change depended on climate change or the COVID-19 pandemic. The main parameters that influenced habitat change were the general increase of temperature and the overall decrease of dissolved oxygen and chlorophyll-a. Although the observed temperature and DOX trends depend on climate change, the chlorophyll-a decrease in 2020 was likely a consequence of the COVID-19 pandemic.

Although some species - *S. solea*, *S. mantis*, and *E. encrasicolus* - were not significantly affected by these changes, heterogeneous effects on the other species habitat were observed. The increasing temperature and decreasing DOX trends - i.e., the potential effects of climate change - negatively affected the distribution of *P. longirostris* by making its habitat overall unstable and less suitable in 2020 than in 2019. This potential negative dependency on climate change finds confirmation by several studies on this species (Colloca et al., 2014; Quattrocchi et al., 2020; Sbrana et al., 2019; Ungaro and Gramolini, 2006). Conversely, these trends favoured *S. officinalis* and extended its potential habitat, in agreement with other studies that analysed its response to the single parameter changes (Capaz et al., 2017; Palmegiano and d'Apote, 1983).

The potential coupling between climate change and COVID-19 - manifested as a simultaneous decreasing trend of DOX and chlorophyll-a - negatively affected the distribution of *S. pilchardus*. Other studies have also reported habitat instability of this species' habitat as the consequence of the variation of these parameters (Ganias, 2009; Sinovčić, 2001). However, the combination of rising temperature and decreasing chlorophyll-a positively affected the habitats of *M. merluccius* and *M. barbatus*. This observation agrees with parameter-specific indications by other studies (García-Rodríguez et al., 2011; Gucu and Bingel, 2011; Sabates et al., 2015; Sion et al., 2019). These two species were the major beneficiary of the two parameter trend combination. Thus, reduced anthropogenic stress on ecosystems in 2020 was beneficial for some species' habitats.

4.1. Reusability and limitations of the approach

Our approach predicted potential general consequences of climate change on species habitat and its coupling with the COVID-19 pandemic. In this view, it can be useful for integrated environmental assessments (Antunes and Santos, 1999; Kristensen, 2004). For example, it can be combined with human activity analysis and when estimating available biomass, and can be used in models that predict risk of regime shift caused by habitat loss (Deyoung et al., 2008; Graham et al., 2015; Wernberg et al., 2016). Notably, the potential effects of reduced fishing activity - due to sanitary restrictions and market closure - on habitat distributions are yet unclear. Only a 10% reduction of fishing hours with

respect to the 2019 level has been estimated globally (for large and small scale fisheries) (Clavelle, 2020; WWF, 2020). Furthermore, the overall fishing activity reduction was just 4% in the Italian seas (Clavelle, 2020). Such a low reduction possibly had minor effects on the habitat distributions of our analysed species and will be the subject of our future investigations. Our approach is also general enough to be applied to other species and areas. To this aim, our workflow uses FAIR data that have a global-scale coverage. Furthermore, our software is open source, and all data are reported under the ESRI-grid format (see Supplementary Material). Specifically, the optimal MaxEnt models and the data are all available as raster ESRI-grid files in the repository linked in the Supplementary Material, within the "Phase 4 - MaxEnt Re-application/ MaxEnt Distributions and Statistics" folder, for re-use in GIS software and other experiments.

The main limitation of our experiment is the low amount of data used, due to current data availability, which was partially compensated by accurate data selection and model optimisation. Although the proposed Adriatic-scale pattern analysis is reliable enough to extract habitat change trends, the produced maps cannot be considered punctually reliable (Queiroz et al., 2021). Conducting a precise analysis will require collecting, collating, and analysing a massive amount of data that will be available only years after the end of the pandemic. Nevertheless, data-poor approaches like ours can predict realistic macroscopic patterns and indicate priority directions for investigating species modifications in the search for confirmation or confutation of the reported results (Coro et al., 2015b, 2016a). In this view, our model allows looking ahead to the possible significant modifications that will possibly be observed in the Adriatic in the following years due to the impact of the combined action of the COVID-19 pandemic and climate change on species distributions. Small-scale reliability can also be enhanced in our model when marine environmental data and species records will be more dense and uniform in the study area. Several initiatives are promoting the collection of these data (EU Commission, 2020a; EU Commission, 2020b; Snapshot-CNR, 2020), but they are ongoing and main address regional scales. These data will be a fundamental source of information to repeat our analysis and validate its predictions. We believe that these activities are justified to understand the effects of natural and man-made pressure on marine ecosystems in current and future scenarios. Our study also confirmed that in order to realise the UN Decade on Ecosystem Restoration motto "the science we need for the ocean we want" (United Nations, 2021b) an Open Science approach can be successful.

Declaration of Competing Interest

The authors declare that they have no known competing financial interests or personal relationships that could have appeared to influence the work reported in this paper.

Acknowledgments

The authors acknowledge Enrico Nicola Armelloni and Giuseppe Scarcella for indications about Adriatic fisheries. This research was partially funded by the SNAPSHOT project of the National Research Council of Italy (CNR) and by the Blue Cloud EU Project (Grant Agreement No. 862409).

Appendix A. Supplementary data

Supplementary data to this article can be found online at https://doi.org/10.1016/j.ecoinf.2022.101675.

References

Adwibowo, A., 2020. Does social distancing have an effect on water quality? An evidence from chlorophyll-a level in the water of populated southeast asian coasts. https://www.preprints.org/manuscript/202005.0091/v1/download.
Alvera-Azcárate, A., Barth, A., Rixen, M., Beckers, J.M., 2005. Reconstruction of incomplete oceanographic data sets using empirical orthogonal functions: application to the adriatic sea surface temperature. Ocean Model 9, 325–346.
Angeletti, L., Prampolini, M., Foglini, F., Grande, V., Taviani, M., 2020. Cold-water coral habitat in the bari canyon system, southern adriatic sea (mediterranean sea). In: Seafloor Geomorphology as Benthic Habitat. Elsevier, pp. 811–824.
Antunes, P., Santos, R., 1999. Integrated environmental management of the oceans. Ecol. Econ. 31, 215–226.
AquaMaps, 2020. AquaMaps Web Site. http://www.aquamaps.org.
Araujo, M.B., Naimi, B., 2020. Spread of Sars-Cov-2 Coronavirus Likely to Be Constrained by Climate. https://doi.org/10.1101/2020.03.12.20034728 preprint.
Ardizzone, G., Gravina, M., Belluscio, A., Schintu, P., 1990. Depth-size distribution pattern of parapenaeus longirostris (Lucas, 1846)(decapoda) in the central mediterranean sea. J. Crustac. Biol. 10, 139–147.
Argo, 2000. Argo float data and metadata from global data assembly centre (argo gdac). SEANOE. https://doi.org/10.17882/42182.
Arif, M., Kumar, R., Parveen, S., Verma, N., 2020. Reduction in water pollution in yamuna river due to lockdown under COVID-19 pandemic. Pharma Innov. J. 9, 84–89.
Arnold, T.W., 2010. Uninformative parameters and model selection using akaike's information criterion. J. Wildl. Manag. 74, 1175–1178.
Ashraf, U., Peterson, A.T., Chaudhry, M.N., Ashraf, I., Saqib, Z., Rashid Ahmad, S., Ali, H., 2017. Ecological niche model comparison under different climate scenarios: a case study of olea spp. in asia. Ecosphere 8, e01825.
Assante, M., Candela, L., Castelli, D., Cirillo, R., Coro, G., Frosini, L., Lelii, L., Mangiacrapa, F., Pagano, P., Panichi, G., et al., 2019. Enacting open science by d4science. Futur. Gener. Comput. Syst. 101, 555–563.
Azzolin, M., Arcangeli, A., Cipriano, G., Crosti, R., Maglietta, R., Pietroluongo, G., Saintingan, S., Zampollo, A., Fanizza, C., Carlucci, R., 2020. Spatial distribution modelling of striped dolphin (stenella coeruleoalba) at different geographical scales within the eu adriatic and ionian sea region, central-eastern mediterranean sea. Aquat. Conserv. Mar. Freshwat. Ecosyst. 30, 1194–1207.
Baker, R.E., Peña, J.-M., Jayamohan, J., Jérusalem, A., 2018. Mechanistic models versus machine learning, a fight worth fighting for the biological community? Biol. Lett. 14, 20170660.
Bargain, A., Marchese, F., Savini, A., Taviani, M., Fabri, M.C., 2017. Santa maria di leuca province (mediterranean sea): identification of suitable mounds for cold-water coral settlement using geomorphometric proxies and maxent methods. Front. Mar. Sci. 4, 338.
Barth, A., Alvera-Azcárate, A., Troupin, C., Ouberdous, M., Beckers, J.M., 2010. A web interface for griding arbitrarily distributed in situ data based on data-interpolating variational analysis (diva). Adv. Geosci. 28, 29–37.
Ben Rais Lasram, F., Guilhaumon, F., Albouy, C., Somot, S., Thuiller, W., Mouillot, D., 2010. The mediterranean sea as a 'cul-de-sac'for endemic fishes facing climate change. Glob. Chang. Biol. 16, 3233–3245.
Bennett, A.F., 1992. Inverse Methods in Physical Oceanography. Cambridge University Press.
Blackford, J., 2002. The influence of microphytobenthos on the northern adriatic ecosystem: a modelling study. Estuar. Coast. Shelf Sci. 55, 109–123.
Brown, C., Fulton, E., Hobday, A., Matear, R., Possingham, H., Bulman, C., Christensen, V., Forrest, R., Gehrke, P., Gribble, N., et al., 2010. Effects of climate-driven primary production change on marine food webs: implications for fisheries and conservation. Glob. Chang. Biol. 16, 1194–1212.
Candela, L., Castelli, D., Coro, G., Pagano, P., Sinibaldi, F., 2016. Species distribution modeling in the cloud. Concurr. Comp. Pract. Exp. 28, 1056–1079.
Capaz, J.C., Tunnah, L., MacCormack, T.J., Lamarre, S.G., Sykes, A.V., Driedzic, W.R., 2017. Hypoxic induced decrease in oxygen consumption in cuttlefish (sepia officinalis) is associated with minor increases in mantle octopine but no changes in markers of protein turnover. Front. Physiol. 8, 344.
Capezzuto, F., Sion, L., Ancona, F., Carlucci, R., Carluccio, A., Cornacchia, L., Maiorano, P., Ricci, P., Tursi, A., D'Onghia, G., 2018. Cold-water coral habitats and canyons as essential fish habitats in the southern adriatic and northern ionian sea (central mediterranean). Ecol. Quest. 29, 9–23.
Chala, D., Roos, C., Svenning, J.C., Zinner, D., 2019. Species-specific effects of climate change on the distribution of suitable baboon habitats–ecological niche modeling of current and last glacial maximum conditions. J. Hum. Evol. 132, 215–226.
Chunco, A.J., Phimmachak, S., Sivongxay, N., Stuart, B.L., 2013. Predicting environmental suitability for a rare and threatened species (lao newt, laotriton laoensis) using validated species distribution models. PLoS One 8, e59853.
Clavelle, T., 2020. Global Fisheries during COVID-19. https://globalfishingwatch.org/data-blog/global-fisheries-during-covid-19/.
Cobos, M.E., Peterson, A.T., Barve, N., Osorio-Olvera, L., 2019. Kuenm: an r package for detailed development of ecological niche models using maxent. PeerJ 7, e6281.
Cohen, J., et al., 1960. A coefficient of agreement for nominal scales. Educ. Psychol. Meas. 20, 37–46.

Coll, M., Santojanni, A., Palomera, I., Tudela, S., Arneri, E., 2007. An ecological model of the northern and central adriatic sea: analysis of ecosystem structure and fishing impacts. J. Mar. Syst. 67, 119–154.
Colloca, F., Mastrantonio, G., Lasinio, G.J., Ligas, A., Sartor, P., 2014. *Parapenaeus longirostris* (Lucas, 1846) an early warning indicator species of global warming in the central mediterranean sea. J. Mar. Syst. 138, 29–39. URL.
Coro, G., 2020. A global-scale ecological niche model to predict sars-cov-2 coronavirus infection rate. Ecol. Model. 431, 109187.
Coro, G., Bove, P., 2022. A high-resolution global-scale model for COVID-19 infection rate. ACM Trans. Spat. Algorithms Syst. (TSAS) 8, 1–24.
Coro, G., Trumpy, E., 2020. Predicting geographical suitability of geothermal power plants. J. Clean. Prod. 267, 121874.
Coro, G., Pagano, P., Ellenbroek, A., 2013a. Automatic procedures to assist in manual review of marine species distribution maps. In: International Conference on Adaptive and Natural Computing Algorithms. Springer, pp. 346–355.
Coro, G., Pagano, P., Ellenbroek, A., 2013b. Combining simulated expert knowledge with neural networks to produce ecological niche models for latimeria chalumnae. Ecol. Model. 268, 55–63.
Coro, G., Pagano, P., Ellenbroek, A., 2014. Comparing heterogeneous distribution maps for marine species. GISci. Rem. Sens. 51, 593–611.
Coro, G., Candela, L., Pagano, P., Italiano, A., Liccardo, L., 2015a. Parallelizing the execution of native data mining algorithms for computational biology. Concurr. Comp. Pract. Exp. 27, 4630–4644.
Coro, G., Magliozzi, C., Ellenbroek, A., Pagano, P., 2015b. Improving data quality to build a robust distribution model for architeuthis dux. Ecol. Model. 305, 29–39.
Coro, G., Webb, T.J., Appeltans, W., Bailly, N., Cattrijsse, A., Pagano, P., 2015c. Classifying degrees of species commonness: North Sea fish as a case study. Ecol. Model. 312, 272–280. URL.
Coro, G., Magliozzi, C., Vanden Berghe, E., Bailly, N., Ellenbroek, A., Pagano, P., 2016a. Estimating absence locations of marine species from data of scientific surveys in obis. Ecol. Model. 323, 61–76. URL. https://www.sciencedirect.com/science/article/pii/S0304380015005761. https://doi.org/10.1016/j.ecolmodel.2015.12.008.
Coro, G., Pagano, P., Napolitano, U., 2016b. Bridging environmental data providers and seadatanet diva service within a collaborative and distributed e-infrastructure. Bollettino di Geofisica 23–25.
Coro, G., Magliozzi, C., Ellenbroek, A., Kaschner, K., Pagano, P., 2016c. Automatic classification of climate change effects on marine species distributions in 2050 using the aquamaps model. Environ. Ecol. Stat. 23, 155–180.
Coro, G., Panichi, G., Scarponi, P., Pagano, P., 2017. Cloud computing in a distributed e-infrastructure using the web processing service standard. Concurr. Comp. Pract. Exp. 29, e4219.
Coro, G., Pagano, P., Ellenbroek, A., 2018a. Detecting patterns of climate change in long-term forecasts of marine environmental parameters. Int. J. Digit. Earth 1–19.
Coro, G., Scarponi, P., Pagano, P., 2018b. Enhancing Argo floats data re-usability. Bollettino di Geofisica 53.
Coro, G., Vilas, L.G., Magliozzi, C., Ellenbroek, A., Scarponi, P., Pagano, P., 2018c. Forecasting the ongoing invasion of lagocephalus sceleratus in the mediterranean sea. Ecol. Model. 371, 37–49.
Coro, G., Pagano, P., Ellenbroek, A., 2020. Detecting patterns of climate change in long-term forecasts of marine environmental parameters. Int. J. Digit. Earth 13, 567–585.
Coro, G., Ellenbroek, A., Pagano, P., 2021. An open science approach to infer fishing activity pressure on stocks and biodiversity from vessel tracking data. Ecol. Inform. 64, 101384.
Coro, G., Tassetti, A.N., Armelloni, E.N., Pulcinella, J., Ferrà, C., Sprovieri, M., Trincardi, F., Scarcella, G., 2022. COVID-19 lockdowns reveal the resilience of adriatic sea fisheries to forced fishing effort reduction. Sci. Rep. 12, 1–14.
Corsi, F., de Leeuw, J., Skidmore, A., 2000. Modeling Species Distribution with GIS. Research Techniques in Animal Ecology. Columbia University Press, New York, pp. 389–434.
de Siqueira, M.F., Durigan, G., de Marco Júnior, P., Peterson, A.T., 2009. Something from nothing: using landscape similarity and ecological niche modeling to find rare plant species. J. Nat. Conserv. 17, 25–32.
Deneu, B., Servajean, M., Bonnet, P., Botella, C., Munoz, F., Joly, A., 2021. Convolutional neural networks improve species distribution modelling by capturing the spatial structure of the environment. PLoS Comput. Biol. 17, e1008856.
Depellegrin, D., Bastianini, M., Fadini, A., Menegon, S., 2020. The effects of COVID-19 induced lockdown measures on maritime settings of a coastal region. Sci. Total Environ. 740, 140123.
Deyoung, B., Barange, M., Beaugrand, G., Harris, R., Perry, R.I., Scheffer, M., Werner, F., 2008. Regime shifts in marine ecosystems: detection, prediction and management. Trends Ecol. Evol. 23, 402–409.
Djakovac, T., Supić, N., Aubry, F.B., Degobbis, D., Giani, M., 2015. Mechanisms of hypoxia frequency changes in the northern adriatic sea during the period 1972–2012. J. Mar. Syst. 141, 179–189.
DownToEarth. Upper Oceans Hottest in 2020 Despite Lower Emissions Due to COVID-19 Lockdowns. http://www.downtoearth.org.in/news/climate-change/upper-oceans-hottest-in-2020-despite-lower-emissions-due-to-covid-19-lockdowns-75056.
Dudík, M., Phillips, S., Schapire, R.E., 2005. Correcting sample selection bias in maximum entropy density estimation. Adv. Neural Inf. Proces. Syst. 18, 323–330.
Durand, M., Fu, L.L., Lettenmaier, D.P., Alsdorf, D.E., Rodriguez, E., Esteban-Fernandez, D., 2010. The surface water and ocean topography mission: observing terrestrial surface water and oceanic submesoscale eddies. Proc. IEEE 98, 766–779.
Elith, J., Graham, C.H., 2009. Do they? How do they? Why do they differ? On finding reasons for differing performances of species distribution models. Ecography 32, 66–77.
Elith, J., Phillips, S.J., Hastie, T., Dudík, M., Chee, Y.E., Yates, C.J., 2011. A statistical explanation of maxent for ecologists. Divers. Distrib. 17, 43–57.
Esposito, V., Andaloro, F., Bianca, D., Natalotto, A., Romeo, T., Scotti, G., Castriota, L., 2014. Diet and prey selectivity of the red mullet, *mullus barbatus* (pisces: Mullidae), from the southern tyrrhenian sea: the role of the surf zone as a feeding ground. Mar. Biol. Res. 10, 167–178.
EU Commission, 2020a. A European Green Deal. https://ec.europa.eu/info/strategy/priorities-2019-2024/european-green-deal.
EU Commission, 2020b. Mission Starfish 2030: Restore our Ocean and Waters. https://ec.europa.eu/info/publications/mission-starfish-2030-restore-our-ocean-and-waters_en.
FAO, 2020. The State of Mediterranean and Black Sea Fisheries 2020. https://doi.org/10.4060/cb2429en.
Friedlaender, A.S., Johnston, D.W., Fraser, W.R., Burns, J., Costa, D.P., et al., 2011. Ecological niche modeling of sympatric krill predators around marguerite bay, western antarctic peninsula. In: Deep Sea Research Part II: Topical Studies in Oceanography, pp. 1729–1740.
Froese, R., Winker, H., Coro, G., Demirel, N., Tsikliras, A.C., Dimarchopoulou, D., Scarcella, G., Quaas, M., Matz-Lück, N., 2018. Status and rebuilding of european fisheries. Mar. Policy 93, 159–170.
Ganias, K., 2009. Linking sardine spawning dynamics to environmental variability. Estuar. Coast. Shelf Sci. 84, 402–408.
Garcia, D.A., Amori, M., Giovanardi, F., Piras, G., Groppi, D., Cumo, F., De Santoli, L., 2019. An identification and a prioritisation of geographic and temporal data gaps of mediterranean marine databases. Sci. Total Environ. 668, 531–546.
García-Rodríguez, M., Fernández, A., Esteban, A., 2011. Biomass response to environmental factors in two congeneric species of mullus, m. barbatus and m. surmuletus, off catalano–levantine mediterranean coast of Spain: a preliminary approach. Anim. Biodivers. Conserv. 34, 113–122.
GEBCO, 2020. Gridded Bathymetry Data. https://www.gebco.net/data_and_products/gridded_bathymetry_data/.
GFCM, 2020. Geographical Subareas of the General Fisheries Commission for the Mediterranean. http://www.fao.org/gfcm/data/maps/gsas/en/.
Graham, N.A., Jennings, S., MacNeil, M.A., Mouillot, D., Wilson, S.K., 2015. Predicting climate-driven regime shifts versus rebound potential in coral reefs. Nature 518, 94–97.
Grassle, J., 2000. The ocean biogeographic information system (OBIS): an on-line, worldwide atlas for accessing, modeling and mapping marine biological data in a multidimensional geographic context. Oceanography-Washington Dc-Oceanogr. Soc. 13, 5–7.
Gucu, A., Bingel, F., 2011. Hake, *merluccius merluccius* l., in the northeastern mediterranean sea: a case of disappearance. J. Appl. Ichthyol. 27, 1001–1012.
Guo, Q., Liu, Y., 2010. Modeco: an integrated software package for ecological niche modeling. Ecography 33, 637–642.
Guthery, F.S., Brennan, L.A., Peterson, M.J., Lusk, J.J., 2005. Information theory in wildlife science: critique and viewpoint. J. Wildl. Manag. 69, 457–465.
Hengl, T., Sierdsema, H., Radović, A., Dilo, A., 2009. Spatial prediction of species' distributions from occurrence-only records: combining point pattern analysis, enfa and regression-kriging. Ecol. Model. 220, 3499–3511.
Huang, Y.P., Kao, L.J., Sandnes, F.E., 2008. Efficient mining of salinity and temperature association rules from Argo data. Expert Syst. Appl. 35, 59–68.
Jones, M.C., Dye, S.R., Pinnegar, J.K., Warren, R., Cheung, W.W., 2012. Modelling commercial fish distributions: prediction and assessment using different approaches. Ecol. Model. 225, 133–145.
Justić, D., Legović, T., Rottini-Sandrini, L., 1987. Trends in oxygen content 1911–1984 and occurrence of benthic mortality in the northern adriatic sea. Estuar. Coast. Shelf Sci. 435–445. URL. https://www.sciencedirect.com/science/article/pii/0272771487900357. https://doi.org/10.1016/0272-7714(87)90035-7.
Kaschner, K., Watson, R., Trites, A., Pauly, D., 2006. Mapping world-wide distributions of marine mammal species using a relative environmental suitability (res) model. Mar. Ecol. Prog. Ser. 316, 285–310.
Kaschner, K., Ready, J., Agbayani, E., Kesner-Reyes, K., Rius-Barile, J., Eastwood, P., South, A., Kullander, S., Rees, T., Watson, R., et al., 2011. Using 'aquamaps' for representing species distribution in regional seas. In: Fisheries Centre Research Reports. Fisheries Centre, University of British Columbia, pp. 17–21.
Kemp, P.S., Froese, R., Pauly, D., 2020. COVID-19 provides an opportunity to advance a sustainable Uk fisheries policy in a post-brexit brave new world. Mar. Policy 120, 104114.
Kralj, M., Lipizer, M., Čermelj, B., Celio, M., Fabbro, C., Brunetti, F., Francé, J., Mozetič, P., Giani, M., 2019. Hypoxia and dissolved oxygen trends in the northeastern adriatic sea (gulf of Trieste). Deep-Sea Res. II Top. Stud. Oceanogr. 164, 74–88.
Kralj, M., Lipizer, M., Čermelj, B., Celio, M., Fabbro, C., Brunetti, F., Francé, J., Mozetič, P., Giani, M., 2019b. Hypoxia and dissolved oxygen trends in the northeastern adriatic sea (gulf of trieste). Deep-Sea Res. II Top. Stud. Oceanogr. 164, 74–88. URL. https://www.sciencedirect.com/science/article/pii/S096706451930013X. https://doi.org/10.1016/j.dsr2.2019.06.002. Revisiting the Eastern Mediterranean: Recent knowledge on the physical, biogeochemical and ecosystemic states and trends (Volume I).
Kristensen, P., 2004. The DPSIR Framework, European Topic Centre on Water. European Environment Agency, pp. 1–10.
Landis, J.R., Koch, G.G., 1977. The measurement of observer agreement for categorical data. Biometrics 159–174.
Le Quéré, C., Jackson, R.B., Jones, M.W., Smith, A.J., Abernethy, S., Andrew, R.M., De-Gol, A.J., Willis, D.R., Shan, Y., Canadell, J.G., et al., 2020. Temporary reduction in

daily global co 2 emissions during the COVID-19 forced confinement. Nat. Clim. Chang. 10, 647–653.
Lipizer, M., Partescano, E., Rabitti, A., Giorgetti, A., Crise, A., 2014. Qualified temperature, salinity and dissolved oxygen climatologies in a changing adriatic sea. Ocean Sci. 10, 771–797.
Magliozzi, C., Coro, G., Grabowski, R.C., Packman, A.I., Krause, S., 2019. A multiscale statistical method to identify potential areas of hyporheic exchange for river restoration planning. Environ. Model. Softw. 111, 311–323.
Marasović, I., Ninčević, Ž., Kušpilić, G., Marinović, S., Marinov, S., 2005. Long-term changes of basic biological and chemical parameters at two stations in the middle adriatic. J. Sea Res. 54, 3–14.
Menchetti, M., Guéguen, M., Talavera, G., 2019. Spatio-temporal ecological niche modelling of multigenerational insect migrations. Proc. R. Soc. B 286, 20191583.
Merow, C., Smith, M.J., Silander Jr., J.A., 2013. A practical guide to maxent for modeling species' distributions: what it does, and why inputs and settings matter. Ecography 36, 1058–1069.
Mishra, D.R., Kumar, A., Muduli, P.R., Equeenuddin, S.M., Rastogi, G., Acharyya, T., Swain, D., 2020. Decline in phytoplankton biomass along indian coastal waters due to COVID-19 lockdown. Remote Sens. 12 https://doi.org/10.3390/rs12162584.
Morales, N.S., Fernández, I., Baca-González, V., 2017. Maxent's parameter configuration and small samples: are we paying attention to recommendations? A systematic review. PeerJ 5, e3093.
Muscarella, R., Galante, P.J., Soley-Guardia, M., Boria, R.A., Kass, J.M., Uriarte, M., Anderson, R.P., 2014. Enm eval: an r package for conducting spatially independent evaluations and estimating optimal model complexity for maxent ecological niche models. Methods Ecol. Evol. 5, 1198–1205.
O'Brien, P.C., 1980. The quartiles of the maximum entropy distribution. Econ. Lett. 6, 49–52.
OSGeo, 2019. GDAL - Geospatial Data Abstraction Library. https://www.gdal.org/.
Palmegiano, G., d'Apote, M., 1983. Combined effects of temperature and salinity on cuttlefish (sepia officinalis l.) hatching. Aquaculture 35, 259–264.
Pearson, R.G., 2007. Species' distribution modeling for conservation educators and practitioners. Synthes. Am. Museum Nat. Hist. 50, 54–89.
Peterson, A.T., 2001. Predicting Species' geographic distributions based on ecological niche modeling. Condor 103, 599–605. https://doi.org/10.1093/condor/103.3.599.
Peterson, A.T., 2003. Predicting the geography of species' invasions via ecological niche modeling. Q. Rev. Biol. 78, 419–433.
Peterson, T., Papeş, M., Eaton, M., 2007. Transferability and model evaluation in ecological niche modeling: a comparison of garp and maxent. Ecography 30, 550–560.
Phillips, S.J., Dudík, M., 2008. Modeling of species distributions with maxent: new extensions and a comprehensive evaluation. Ecography 31, 161–175.
Phillips, S.J., Anderson, R.P., Schapire, R.E., 2006a. Maximum entropy modeling of species geographic distributions. Ecol. Model. 190, 231–259.
Phillips, S.J., Anderson, R.P., Schapire, R.E., 2006b. Maximum entropy modeling of species geographic distributions. Ecol. Model. 190, 231–259. URL. http://www.sciencedirect.com/science/article/pii/S030438000500267X.
Phillips, S.J., Anderson, R.P., Dudík, M., Schapire, R.E., Blair, M.E., 2017. Opening the black box: an open-source release of maxent. Ecography 40, 887–893.
Phillips, S., Dudik, M., Schapire, R., 2021. Maxent Software for Modeling Species Niches and Distributions (Version 3.4.1). http://biodiversityinformatics.amnh.org/open_source/maxent/.
Quattrocchi, F., Fiorentino, F., Lauria, V., Garofalo, G., 2020. The increasing temperature as driving force for spatial distribution patterns of parapenaeus longirostris (Lucas 1846) in the strait of sicily (central mediterranean sea). J. Sea Res. 158, 101871. URL.
Queiroz, N., Humphries, N.E., Couto, A., Vedor, M., Da Costa, I., Sequeira, A.M., Mucientes, G., Santos, A.M., Abascal, F.J., Abercrombie, D.L., et al., 2021. Reply to: caution over the use of ecological big data for conservation. Nature 595, E20–E28.
Ravdas, M., Zacharioudaki, A., Korres, G., 2018. Implementation and validation of a new operational wave forecasting system of the mediterranean monitoring and forecasting Centre in the framework of the copernicus marine environment monitoring service. Nat. Hazards Earth Syst. Sci. 18, 2675–2695.
Raybaud, V., Beaugrand, G., Dewarumez, J.M., Luczak, C., 2015. Climate-induced range shifts of the american jackknife clam ensis directus in europe. Biol. Invasions 17, 725–741.
Ready, J., Kaschner, K., South, A.B., Eastwood, P.D., Rees, T., Rius, J., Agbayani, E., Kullander, S., Froese, R., 2010. Predicting the distributions of marine organisms at the global scale. Ecol. Model. 221, 467–478.
Rees, T., 2008. 18.9. Using aquamaps for biodiversity assessment, including a prototype mpa (marine protected area) network design tool. In: The Proceedings of TDWG, 73.
Renner, I.W., Warton, D.I., 2013. Equivalence of maxent and poisson point process models for species distribution modeling in ecology. Biometrics 69, 274–281.
Reside, A.E., Critchell, K., Crayn, D.M., Goosem, M., Goosem, S., Hoskin, C.J., Sydes, T., Vanderduys, E.P., Pressey, R.L., 2019. Beyond the model: expert knowledge improves predictions of species' fates under climate change. Ecol. Appl. 29, e01824.
Reyes, K., 2015. AquaMaps: Algorithm and Data Sources for Aquatic Organisms. https://pacific-data.sprep.org/system/files/AquaMaps_Algorithm_and_Data_Sources.pdf.
Roy-Dufresne, E., Saltré, F., Cooke, B.D., Mellin, C., Mutze, G., Cox, T., Fordham, D.A., 2019. Modeling the distribution of a wide-ranging invasive species using the sampling efforts of expert and citizen scientists. Ecol. Evolut. 9, 11053–11063.
Russo, E., Monti, M.A., Mangano, M.C., Raffaeta, A., Sara, G., Silvestri, C., Pranovi, F., 2020. Temporal and spatial patterns of trawl fishing activities in the adriatic sea (central mediterranean sea, gsa17). Ocean Coast. Manag. 192, 105231.
Sabates, A., Zaragoza, N., Raya, V., 2015. Distribution and feeding dynamics of larval red mullet (*Mullus barbatus*) in the NW Mediterranean: the important role of cladocera. J. Plankton Res. 37, 820–833. https://doi.org/10.1093/plankt/fbv040.
Sánchez-Tapia, A., de Siqueira, M.F., Lima, R.O., Barros, F.S.M., Gall, G.M., Gadelha, L. M., da Silva, L.A.E., Osthoff, C., 2017. Model-r: a framework for scalable and reproducible ecological niche modeling. In: Latin American High Performance Computing Conference. Springer, pp. 218–232.
Santos, A.M.P., Ré, P., Dos Santos, A., Peliz, Á., 2006. Vertical distribution of the european sardine (sardina pilchardus) larvae and its implications for their survival. J. Plankton Res. 28, 523–532.
Sbrana, M., Zupa, W., Ligas, A., Capezzuto, F., Chatzispyrou, A., Follesa, M.C., Gancitano, V., Guijarro, B., Isajlovic, I., Jadaud, A., et al., 2019. Spatiotemporal abundance pattern of deep-water rose shrimp, parapenaeus longirostris, and Norway lobster, nephrops norvegicus, in european mediterranean waters. Sci. Mar. 83, 71–80.
Scarponi, P., Coro, G., Pagano, P., 2018. A collection of aquamaps native layers in netcdf format. Data Brief 17, 292–296.
Schaap, D.M., Lowry, R.K., 2010. Seadatanet–pan-european infrastructure for marine and ocean data management: unified access to distributed data sets. Int. J. Digit. Earth 3, 50–69.
Schnase, J.L., Carroll, M.L., Gill, R.L., Tamkin, G.S., Li, J., Strong, S.L., Maxwell, T.P., Aronne, M.E., Spradlin, C.S., 2021. Toward a Monte Carlo approach to selecting climate variables in maxent. PLoS One 16, e0237208.
Schulzweida, U., 2020. CDO User Guide. https://code.mpimet.mpg.de/projects/cdo/embedded/index.html#x1-5710002.12.6.
Shehhi, M.R.A., Samad, Y.A., 2021. Effects of the COVID-19 pandemic on the oceans. Rem. Sens. Lett. 12, 325–334. https://doi.org/10.1080/2150704X.2021.1880658.
Sinovčić, G., 2001. Biotic and abiotic factors influencing sardine, sardina pilchardus (walb.) abundance in the croatian part of the Eastern Adriatic. In: FAO Adriamed Paper.
Sion, L., Zupa, W., Calculli, C., Garofalo, G., Hidalgo, M., Jadaud, A., Lefkaditou, E., Ligas, A., Peristeraki, P., Bitetto, I., et al., 2019. Spatial distribution pattern of european hake, *merluccius merluccius* (pisces: Merlucciidae), in the mediterranean sea. Sci. Mar. 83, 21–32.
Snapshot-CNR, 2020. Synoptic Assessment of Human Pressures on Key Mediterranean Hot Spots: The Snapshot-CNR Project. http://snapshot.cnr.it.
Tanhua, T., Pouliquen, S., Hausman, J., O'brien, K., Bricher, P., De Bruin, T., Buck, J.J., Burger, E.F., Carval, T., Casey, K.S., et al., 2019. Ocean fair data services. Front. Mar. Sci. 6, 440.
Theil, H., 1982. Some recent and new results on the maximum entropy distribution. Stat. Prob. Lett. 1, 17–22.
Toonen, H.M., Bush, S.R., 2020. The digital frontiers of fisheries governance: fish attraction devices, drones and satellites. J. Environ. Policy Plan. 22, 125–137.
Trifonova, N., Maxwell, D., Pinnegar, J., Kenny, A., Tucker, A., 2017. Predicting ecosystem responses to changes in fisheries catch, temperature, and primary productivity with a dynamic bayesian network model. ICES J. Mar. Sci. 74, 1334–1343.
Troupin, C., Machin, F., Ouberdous, M., Sirjacobs, D., Barth, A., Beckers, J.M., 2010. High-resolution climatology of the Northeast Atlantic using data-interpolating variational analysis (diva). J. Geophys. Res. Oceans 115.
Troupin, C., Barth, A., Sirjacobs, D., Ouberdous, M., Brankart, J.M., Brasseur, P., Rixen, M., Alvera-Azcárate, A., Belounis, M., Capet, A., et al., 2012. Generation of analysis and consistent error fields using the data interpolating variational analysis (diva). Ocean Model 52, 90–101.
Ungaro, N., Gramolini, R., 2006. Possible effect of bottom temperature on distribution of parapenaeus longirostris (Lucas, 1846) in the southern adriatic (mediterranean sea). Turk. J. Fish. Aquat. Sci. 6.
United Nations, 2021a. Cooling La Niña is on the Wane, but Temperatures Set to Rise: UN Weather Agency. https://news.un.org/en/story/2021/02/1084222.
United Nations, 2021b. UN Decade on Ecosystem Restoration. https://www.decadeonrestoration.org/.
Von Schuckmann, K., Le Traon, P.Y., Smith, N., Pascual, A., Brasseur, P., Fennel, K., Djavidnia, S., Aaboe, S., Fanjul, E.A., Autret, E., et al., 2018. Copernicus marine service ocean state report. J. Operation. Oceanogr. 11, S1–S142.
Wang, L., Kerr, L.A., Record, N.R., Bridger, E., Tupper, B., Mills, K.E., Armstrong, E.M., Pershing, A.J., 2018. Modeling marine pelagic fish species spatiotemporal distributions utilizing a maximum entropy approach. Fish. Oceanogr. 27, 571–586.
Warren, D.L., Seifert, S.N., 2011. Ecological niche modeling in maxent: the importance of model complexity and the performance of model selection criteria. Ecol. Appl. 21 (2), 335–342.
Watelet, S., Back, Ö., Barth, A., Beckers, J.M., 2016. Data-interpolating variational analysis (diva) software: recent development and application. In: Proceedings of the EGU General Assembly 2016, European Geosciences Union General Assembly, p. 1.
Weatherdon, L.V., Magnan, A.K., Rogers, A.D., Sumaila, U.R., Cheung, W.W., 2016. Observed and projected impacts of climate change on marine fisheries, aquaculture, coastal tourism, and human health: an update. Front. Mar. Sci. 48.
Weber, M.M., Stevens, R.D., Diniz-Filho, J.A.F., Grelle, C.E.V., 2017. Is there a correlation between abundance and environmental suitability derived from ecological niche modelling? A meta-analysis. Ecography 40, 817–828.
Werdell, P.J., Bailey, S.W., 2005. An improved in-situ bio-optical data set for ocean color algorithm development and satellite data product validation. Remote Sens. Environ. 98, 122–140.
Wernberg, T., Bennett, S., Babcock, R.C., De Bettignies, T., Cure, K., Depczynski, M., Dufois, F., Fromont, J., Fulton, C.J., Hovey, R.K., et al., 2016. Climate-driven regime shift of a temperate marine ecosystem. Science 353, 169–172.

World Meterological Organization, 2021. Climate change indicators and impacts worsened in 2020. https://public.wmo.int/en/media/press-release/climate-change-indicators-and-impacts-worsened-2020.
WWF, 2020. World Wide Fund for Nature - Impact of COVID-19 on Mediterranean Fisheries. https://www.wwfmmi.org/what_we_do/fisheries/transforming_small_scale_fisheries/impact_of_covid_on_mediterranean_fisheries/.
Yunus, A.P., Masago, Y., Hijioka, Y., 2020. COVID-19 and surface water quality: improved lake water quality during the lockdown. Sci. Total Environ. 731, 139012.
Zaniewski, A.E., Lehmann, A., Overton, J.M., 2002. Predicting species spatial distributions using presence-only data: a case study of native New Zealand ferns. Ecol. Model. 157, 261–280.
Zavatarelli, M., Raicich, F., Bregant, D., Russo, A., Artegiani, A., 1998. Climatological biogeochemical characteristics of the adriatic sea. J. Mar. Syst. 18, 227–263. URL. https://www.sciencedirect.com/science/article/pii/S0924796398000141. https://doi.org/10.1016/S0924-7963(98)00014-1.
Zeng, Y., Low, B.W., Yeo, D.C., 2016. Novel methods to select environmental variables in maxent: a case study using invasive crayfish. Ecol. Model. 341, 5–13.
Zhang, G., Zhu, A.X., Windels, S.K., Qin, C.Z., 2018. Modelling species habitat suitability from presence-only data using kernel density estimation. Ecol. Indic. 93, 387–396.